UCSF
UC San Francisco Previously Published Works

Title

Discovery of nitrate–CPK–NLP signalling in central nutrient–growth networks

Permalink

Journal

ISSN

Authors

Liu, Kun-hsiang
Niu, Yajie
Konishi, Mineko
et al.

Publication Date

DOI

Peer reviewed

Discovery of nitrate-CPK-NLP signalling in central nutrient-growth networks

Kun-hsiang Liu[1,4,*], **Yajie Niu**[1,*], **Mineko Konishi**[2], **Yue Wu**[1], **Hao Du**[1], **Hoo Sun Chung**[1], **Lei Li**[1], **Marie Boudsocq**[1,5], **Matthew McCormack**[1], **Shugo Maekawa**[2], **Tetsuya Ishida**[2], **Chao Zhang**[3], **Kevan Shokat**[3], **Shuichi Yanagisawa**[2], and **Jen Sheen**[1]

[1]Department of Molecular Biology and Centre for Computational and Integrative Biology, Massachusetts General Hospital, and Department of Genetics, Harvard Medical School, Boston, MA 02114, USA

[2]Biotechnology Research Center, The University of Tokyo, Yayoi 1-1-1, Bunkyo-ku, Tokyo 113-8657, Japan

[3]Howard Hughes Medical Institute and Department of Cellular and Molecular Pharmacology, UCSF, 600 16th St., San Francisco, California 94143, USA

[4]Basic Forestry and Proteomics Research Center, Fujian Agriculture and Forestry University, Fuzhou, Fujian 350002, China

[5]Institute of Plant Sciences Paris-Saclay (IPS2), CNRS, INRA, Université Paris-Sud, Université d'Evry Val d'Essonne, Université Paris-Diderot, Sorbonne Paris-Cité, Université Paris-Saclay, Bâtiment 630, 91405 Orsay, France

Abstract

Nutrient signalling integrates and coordinates gene expression, metabolism and growth. However, its primary molecular mechanisms remain incompletely understood in plants and animals. Here we report novel Ca^{2+} signalling triggered by nitrate with live imaging of an ultrasensitive biosensor in *Arabidopsis* leaves and roots. A nitrate-sensitized and targeted functional genomic screen identifies subgroup III Ca^{2+}-sensor protein kinases (CPKs) as master regulators orchestrating primary nitrate responses. A chemical switch with the engineered CPK10(M141G) kinase enables conditional analyses of *cpk10,30,32* to define comprehensive nitrate-associated regulatory and developmental programs, circumventing embryo lethality. Nitrate-CPK signalling phosphorylates

---

conserved NIN-LIKE PROTEIN (NLP) transcription factors (TFs) to specify reprogramming of gene sets for downstream TFs, transporters, N-assimilation, C/N-metabolism, redox, signalling, hormones, and proliferation. Conditional *cpk10,30,32* and *nlp7* similarly impair nitrate-stimulated system-wide shoot growth and root establishment. The nutrient-coupled Ca^{2+} signalling network integrates transcriptome and cellular metabolism with shoot-root coordination and developmental plasticity in shaping organ biomass and architecture.

Introduction

Photosynthetic plants are masters in assimilating inorganic chemical resources to organic nutrients that sustain human societies and the food webs of diverse ecosystems. Although sugars derived from plant assimilation of CO_2 and H_2O via photosynthesis contribute to world-wide biomass and agricultural production, nitrogen taken from the soil or air serves as the gatekeeper in integrating C/N nutrient signalling networks and coordinating shoot-root nutrient communications and growth[1–6]. In multicellular organisms, growth factors and hormones are ineffective in growth promotion without the support of C/N nutrient signalling networks[5,7,8]. Surprisingly little is known about the primary nutrient signalling mechanisms in plants and animals beyond the roles of evolutionarily conserved transceptors, target of rapamycin, and AMP-activated protein kinase[2,5–11].

Nitrate is the primary nitrogen source for most plants and the limiting factor for growth in aerobic soil[4,6,12]. Nitrate rapidly stimulates integrated nutrient transport and assimilation, as well as C/N metabolic and regulatory pathways that enable plant growth plasticity to respond and adapt to fluctuating environments. Genetic and genomic evidence suggest that nitrate drives rapid transcriptional regulation and nitrate signalling is uncoupled from nitrate metabolism[1,3,4,9,11–22]. Regulatory components in nitrate sensing and signalling, including the NRT1.1/NPF6.3 transceptor and associated CIPKs (Calcineurin-B-Like-Interacting PKs) and protein phosphatase 2C (PP2C/ABI2), as well as nitrate-responsive *cis*-elements (NRE) and TFs, have been identified with molecular, genetic, genomic and systems analyses[1,3,6,9–25]. Importantly, *Arabidopsis* NLP6 and NLP7 have been implicated as key TFs of primary nitrate responses[12,14,17,18].Despite these advances, the molecular mechanism underlying primary nitrate signalling downstream of multiple sensors to integrated transcription, transport, metabolism and systemic growth programs (Fig. 1a) remains enigmatic[4,6,9–12,16,25].

Ca^{2+} is an evolutionarily conserved and versatile signalling modulator in diverse regulatory pathways, including stress, immune and neuron signalling[26–31]. Although a role of Ca^{2+} signalling in nitrate responsive gene regulation has been implicated in maize leaves and *Arabidopsis* roots[32,33], many outstanding questions remained in both plants and animals, such as whether distinct Ca^{2+} signatures are involved in primary nutrient signalling with cell specificity, the specific patterns of Ca^{2+} dynamics, the identity of intracellular Ca^{2+} sensors, how Ca^{2+} sensors relay signalling specificity, and the downstream targets of Ca^{2+} signalling in the nutrient-growth regulatory networks.

Nitrate triggers unique Ca²⁺-CPK signalling

To elucidate the primary mechanism in nitrate signalling, we developed integrated seedling and cell-based assays in *Arabidopsis*. Without exogenous nitrogen, seed reserves supported rapid initial seedling growth after germination (Fig. 1b). However, the increase in biomass ceased after four days even with illumination and sucrose supplies (Fig. 1c, d). Although NH_4^+ or glutamine (Gln) was transported, sensed and utilized[6,34–35], only nitrate (0.1–10 mM) promoted distinct shoot biomass accumulation and root system architecture establishment. Nitrate, but not metabolites, NH_4^+ or Gln that are derived from nitrate assimilation, sustained substantial postembryonic growth (Fig. 1a, c, d, and Extended Data Fig. 1a), consistent with uncoupling of nitrate signalling from nitrate metabolism[4,13], NH_4^+ or Gln signalling[6,34,35].

Although nitrate-triggered Ca^{2+} signals could be detected using transgenic aequorin seedlings[26,33], the response was subtle when compared with the flg22-induced Ca^{2+} signals in immune signalling (Extended Data Fig. 1b, c). As nitrate signalling and assimilation occur in both leaves and roots (Extended Data Fig. 1a, d, e), we developed a versatile single-cell system to investigate live Ca^{2+} signalling stimulated by nitrate in mesophyll protoplasts[5,17,18,27]. In leaf cells co-expressing the ultrasensitive Ca^{2+} biosensor GCaMP6[36] and a nuclear mCherry, single-cell live recordings revealed that nitrate specifically stimulated a unique and dynamic Ca^{2+} signature in the nucleus and cytosol (Fig. 1e, f). Chelating exogenous Ca^{2+} by EGTA diminished the nitrate-triggered Ca^{2+} signature (Fig. 1f). Unlike the transient and acute $[Ca^{2+}]$cyt increase stimulated by osmotic and cold stresses in seedlings[26,37], nuclear Ca^{2+}oscillation in symbiosis[38], or a 10 sec $[Ca^{2+}]$cyt peak triggered by nitrate in roots[33], a gradually rising subcellular Ca^{2+} signature attributed to nitrate over a course of minutes was recorded by GCaMP6-based imaging with high subcellular resolution. Time-lapse recording using transgenic GCaMP6 plants uncovered a Ca^{2+} signature of similar amplitude and dynamic stimulated by nitrate in mesophyll cells of intact plants (Fig. 1g). Distinct Ca^{2+} dynamics was also triggered by nitrate in the tip, pericycle and stele of intact roots[11,18,20] (Extended Data Fig. 1f, g). To physiologically connect this distinctive Ca^{2+} signature (Supplementary Video 1–4) to established primary nitrate responses, we showed that activation of universal nitrate-responsive marker genes, *NIR* (*NITRITE REDUCTASE*), *G6PD3* (*GLUCOSE-6-PHOSPHATE DEHYDROGENASE3)* and *FNR2 (FERREDOXIN-NADP⁺-OXIDOREDUCTASE2*), was significantly reduced by Gd^{3+} and La^{3+} (blockers of plasma membrane Ca^{2+} channels) or W7 (an intracellular Ca^{2+} sensor inhibitor) (Extended Data Fig. 2a, b) in seedlings[27,32,33]. Our results support a crucial role for nitrate-induced Ca^{2+} signalling in multiple cell types of different tissues and organs.

To search for candidates of intracellular Ca^{2+} sensors mediating primary nitrate signalling, we conducted an in-gel kinase assay and detected enhanced activity of endogenous Ca^{2+}-dependent PKs in response to nitrate within 10 min (Extended Data Fig. 2c). The molecular weight of nitrate-activated PKs was similar to that of most CPKs but not CIPKs[10,22,23,27]. There are 34 *Arabidopsis* CPK genes mediating diverse signalling pathways with complex and redundant functions[27,28,30,39]. As *cpk* mutants have escaped from mutant screens for nitrate signalling[11,16], a simple, rapid and reliable cell-based reporter assay could facilitate

targeted functional genomic screening of CPK candidates involved in nitrate signalling[27]. Using a luciferase (LUC) reporter gene *NIR-LUC* that exhibits a physiological nitrate response in transgenic *Arabidopsis* plants[16], we observed rapid, specific and sensitive regulation of LUC activity by 0.1 to 50 mM KNO_3 within 2 h (Extended Data Fig. 2d-f). Unexpectedly, co-expressing *NIR-LUC* with a constitutively active construct (CPKac)[27] for each of the 25 *CPKs* expressed in mesophyll protoplasts did not trigger marked *NIR-LUC* activation (Fig. 1h). To test the possibility that CPKac-mediated response could be sensitized by low nitrate, we added 0.5 mM KNO_3 to the protoplast incubation medium. Interestingly, subgroup III CPK7/8/10/13/30/32ac were most effective to act synergistically with 0.5 mM KNO_3 for *NIR-LUC* activation (Fig. 1h, i and Extended Data Fig. 2g). Although specific CPKac is sufficient to activate stress or immune responses associated with strong and distinct Ca^{2+} signalling patterns[26–28,30,37], activation of subgroup III CPKac alone did not fully evoke specific nitrate response. Consistent with our findings, it has been suggested that primary nitrate signalling requires the coordination of multiple signalling mechanisms[6,9,10,17,18,40]. Our results indicate that nitrate may specify and synergize functionally redundant subgroup III CPKs in *NIR-LUC* activation.

Chemical switch defines CPK signalling

To test the specificity and physiological roles of subgroup III CPKs, we examined loss-of-function *cpk* mutants. The single *cpk7, cpk8, cpk10, cpk13, cpk30 or cpk32* mutants barely affected nitrate responsive genes and lacked overt growth phenotypes (Extended Data Fig. 3a-g). As CPK10 and CPK30 share the highest sequence identity and slight modulation of *NIR* and *G6PD3* expression (Fig. 1i and Extended Data Fig. 2g, 3d), we attempted to generate the *cpk10,30* double mutant. However, analyses of the siliques revealed that the *cpk10,30* double mutant was lethal at early embryogenesis (Fig. 2a, b).

Aiming to simultaneously overcome embryo lethality and enable analyses of higher-order *cpk* mutants, we engineered CPK10 to be reversibly inhibited by 3MB-PP1-IsoP (3MBiP), a specific and improved derivative of the PK inhibitor PP1 (4-amino-5-(methylphenyl)-7-(t-butyl)pyrazolo-(3,4-d)pyrimidine) (Fig. 2c)[41,42]. A critical determinant of PK inhibitor selectivity is the size of the gatekeeper residue in the ATP-binding pocket[41,42]. By aligning the conserved PK subdomain V in *Arabidopsis* CPK10/30 and human CaMKII, we created the CPK10(M141G) gatekeeper residue mutant (Fig. 2d). Importantly, 3MBiP completely inhibited the kinase activity of CPK10(M141G) but not wild-type (WT) CPK10 (Fig. 2e). A genomic construct expressing CPK10(M141G) was introduced into *cpk10, cpk30/+* to rescue the lethal embryo phenotype of its *cpk10,30* progenies, creating a 3MBiP-inducible *icpk10,30* mutant (Fig. 2a, b). The HA-tagged CPK10(M141G) protein immunoprecipitated from the transgenic plants was completely inhibited by 3MBiP (Fig. 2f). Because CPK32ac greatly enhanced *NIR-LUC* expression (Fig. 1h), we also generated the *cpk10,32* and *cpk30,32* double mutants, as well as the 3MBiP-inducible *icpk10,30,32* triple mutant expressing CPK10(M141G)-HA (designated *icpk*) by genetic crosses and molecular confirmation. Nitrate responsive marker genes showed a reduction in double mutants, including *cpk10,32, cpk30,32* and *icpk10,30* in the presence of 3MBiP (Extended Data Fig. 3i, j) without displaying visible phenotype in plant growth supported by nitrate (Extended Data Fig. 3d, e, g). Expression of nitrate marker genes was further reduced in the 3MBiP-

inducible *icpk* triple mutant (Fig. 2g), correlated with retarded plant growth (Extended Data Fig. 3h). Insensitivity of WT plants to 3MBiP treatment in gene expression and seedling growth (Fig. 2g and Extended Data Fig. 3e, f, h, j) validated the specificity of 3MBiP. By overcoming dual genetic redundancy and embryo lethality, chemical genetics offers a new approach to further elucidate the dynamic and physiological functions of higher-order *cpk* mutants not previously possible.

Nitrate-CPKs control primary transcription

To explore the genome-wide transcriptional landscape controlled by nitrate-CPK signalling, we conducted RNA-seq experiments 15 min after nitrate induction in WT and *icpk* seedlings. In WT seedlings, 394 and 79 genes were activated and repressed, respectively, in response to nitrate ($\log_2$ 1 or −1; *q*-value 0.05), which significantly overlapped with nitrate-responsive genes discovered in microarray-based studies of both roots and shoots[1,13,15,18]. In *icpk*, 266 up-regulated (68%) and 44 down-regulated (56%) genes could be defined as statistically significant nitrate-CPK target genes (*icpk* KNO_3 vs. WT KNO_3, *q*-value 0.05) (Fig. 3, Extended Data Fig. 4, 5 and Supplementary Table 1 and 2). Thus, CPK10/30/32 play a central role in regulating primary nitrate responses in the entire plant system.

Among the statistically significant primary nitrate-CPK target genes, CPK10/30/32 modulated diverse key cellular and metabolic functions immediately activated by nitrate[1,3,4,6,12,13,15,17,18,25]. The most significantly enriched functional classes of genes were those supporting nitrate transport and assimilation; two routes of glucose-6-phosphate metabolism via the oxidative pentose-phosphate pathway (OPP) and glycolysis; amino acid transport and metabolism; other transporters; C/N-metabolism; cytokinin, auxin and abscisic acid (ABA) metabolism and signalling; protein degradation; stress; signalling; and transcription (Fig. 3b, c, Extended Data Fig. 4 and Supplementary Table 1 and 2). Remarkably, the universal nitrate-inducible genes responsible for the conserved nitrogen uptake and assimilation processes from *Arabidopsis*, rice to maize were regulated by CPK10/30/32 (Extended Data Fig. 4e-g)[1,3,4,12,17,18,21,32]. Nearly 50 genes encoding annotated TFs were activated by nitrate via CPK10/30/32 (Supplementary Table 2), providing potential amplification of the downstream nitrate transcriptional network[17,18,20,24,25]. Nitrate-CPK signalling repressed genes were involved in transcription, metabolism and transport (Extended Data Fig. 4b, d and Supplementary Table 2).

We carried out RT-qPCR analyses of primary nitrate-CPK target genes for eight major functional classes, including OPP, nitrate and amino acid transporters, N-metabolism, CHO-metabolism, signalling, cytokinin synthesis, and TFs in WT and *icpk* mutant plants (Extended Data Fig. 4f, g and Supplementary Table 2). Notably, nitrate activation of *CYP735A2* expression to enhance *trans*-zeatin synthesis is critical for shoot development, providing an interconnection between local and systemic nitrate signalling via the action of a mobile growth hormone[43]. As nitrate activation of these marker genes was markedly diminished in the *icpk* mutant, CPK10/30/32 are master regulators in primary nitrate signalling and integrate global gene expression to nitrate-activated metabolic and physiological responses (Fig. 3, Extended Data Fig. 4e-g and Supplementary Table 2).

Nitrate-CPKs dictate growth plasticity

To investigate the nexus between nitrate-specific developmental programs (Fig. 1c, d) and nitrate-CPK signalling, we examined shoot growth by quantifying shoot fresh weight in WT and *icpk* seedlings. To bypass any early effect of nitrate on seed germination, we selected 3-day-old seedlings without apparent phenotypes on ammonium plates and placed them on 3MBiP medium in the presence of KCl, NH_4^+, Gln or KNO_3 for 5–8 days. Although NH_4^+ or Gln could promote limited shoot greening and growth equally in WT and *icpk* seedlings, nitrate was essential for full greening and expansion of cotyledons and true leaves in WT (Fig. 4 and Extended Data Fig. 1a, 6a)[3,16]. The specific *icpk* deficiency of cotyledon and leaf expansion in response to nitrate (Fig. 4a-c) might be partially correlated with reduced expression of *CYP735A2* for *trans*-zeatin synthesis (Extended Data Fig. 4f, g)[43].

We next examined the roles of CPK10/30/32 in nitrate-specific control of the root developmental program. The nitrate-specific stimulation of lateral root primordia density was reduced and lateral root elongation was severely retarded in *icpk* (Fig. 4c and Extended Data Fig. 6). Although ammonium supported lateral root initiation similarly in WT and *icpk* seedlings[6,35], nitrate-CPK signalling was essential for lateral root primordia progression and emergence, as well as lateral root elongation (Fig. 4c and Extended Data Fig. 6c-e). We quantified the dynamic distribution of all lateral roots from primordia stages I-VII to emergence (Em) and fully elongated (LR) stages[44] in WT and *icpk*. The proportion of emerged lateral root (Em+LR) increased from 0% (4 days) to 40% (8 days) after transfer to the nitrate medium, and 3MBiP did not affect normal root system development in WT. In contrast, the *icpk* lateral root primordia were arrested most conspicuously in roots 6–8 days after transfer (Extended Data Fig. 6d-g).

Intriguingly, the primary root length was similar between WT and *icpk* in 8-day-old seedlings on KCl or on different nitrogen media. Thus, the growth of primary roots at the early stage of development immediately after germination relied mainly on the seed nutrient reserves and sugars with limited influence by exogenous nitrogen nutrients (Extended Data Fig. 6a, b)[2,5]. In 11-day-old plants, WT and *icpk* plants were indistinguishable on KCl, NH_4^+ or Gln medium, displaying limited shoot and root growth and development. However, vigorous primary and lateral root growth promoted by exogenous nitrate was abolished in *icpk* (Fig. 1c, d and 4c)[16]. CPK10/30/32 specifically defined the long-term systemic shoot developmental program and root system architecture via modulating the primary nitrate-signalling network[6,16].

The nitrate-CPK-NLP regulatory network

Arabidopsis

NLP6 and NLP7 have been identified as key TFs of primary nitrate responses, but how NLP6/7 are activated by nitrate remains a mystery[6,12–14,17,18,25]. Analyses of transgenic plants revealed a nitrate-stimulated NLP6/7-MYC mobility shift at 5–30 min, which was eliminated by phosphatase (Fig. 5a, b and Extended Data Fig. 7a, b). The nitrate-stimulated NLP7-MYC phosphorylation was greatly diminished by Gd^{3+} and La^{3+} (Fig. 5c), or by W7 (Extended Data Fig. 7c), analogous to the nitrate responsive gene regulation (Extended Data

Fig. 2a, b). Furthermore, CPK10/30/32, but not the kinase-dead CPK10KM or the subgroup I CPK11, phosphorylated NLP7 *in vitro* (Fig. 5d). As the Ca^{2+} chelator EGTA abolished the phosphorylation of NLP7 or histone by CPK10/30/32 but not by CPK10/30/32ac lacking the Ca^{2+}-binding domain[27–30] (Fig. 5e and Extended Data Fig. 7d), CPK10/30/32 were Ca^{2+} sensors and effectors to relay nitrate signalling. The nitrate-CPK-NLP6/7 signalling link was further supported by the significant overlaps between nitrate-CPK and nitrate-NLP6/7 target genes as universal nitrate response marker genes (Fig. 3c, Extended Data Fig. 4, 5 and Supplementary Table 2)[12,17,18].

By aligning nine *Arabidopsis* NLPs and four orthologous *Lotus japonicus* NLPs using integrated computational and literature analyses[12,17,18], we identified a uniquely conserved serine (S205 in NLP7) as a candidate CPK phosphorylation site (Extended Data Fig. 7e). CPK10ac, CPK30ac and CPK32ac phosphorylated the nitrate responsive domain of WT NLP7-N(1–581 a.a.)[17] but not NLP7-N(S205A) (Extended Data Fig. 7f). Moreover, NLP7(S205A) lost nitrate-stimulated phosphorylation in transgenic plants (Extended Data Fig. 7g). Mass spectrometry analyses confirmed that S205 in NLP7 was phosphorylated *in vivo* in the presence of nitrate (Fig. 5f). Like CPK10/30/32ac, NLP7 overexpression but neither kinase-dead CPK10ac(KM) nor NLP7(S205A), acted synergistically with 0.5 mM nitrate to enhance *NIR-LUC* activation (Fig. 1h and Extended Data Fig. 7h). Finally, nitrate-triggered NLP7 phosphorylation at S205 *in vivo* was abolished in the *icpk* mutant (Fig. 5g).

To further validate the nitrate-CPK-NLP link, we discovered nitrate-stimulated rapid nuclear translocation of CPK10-GFP, CPK30-GFP and CPK32-GFP by confocal imaging (Fig. 6a and Extended Data Fig. 8a). Only NLP7-GFP but not NLP7(S205A)-GFP responded to nitrate stimulation with persistent nuclear localization in leaf cells (Fig. 6b) and in the transgenic *nlp7* roots (Extended Data Fig. 8b)[18]. Using *in vivo* Bimolecular Fluorescence Complementation (BiFC) assay, we showed that CPK10KM directly interacted with NLP7 in the nucleus in the presence of nitrate in protoplasts (Fig. 6c). Nitrate stimulated nuclear retention of NLP7-GFP was greatly diminished in *icpk* protoplasts (Fig. 6d). These complementary *in vivo* and *in vitro* analyses provided compelling evidence to support the signalling connections from CPK10/30/32 to NLP phosphorylation in mediating primary nitrate signalling and transcription.

To identify functionally significant NLP7 target genes in the nitrate-CPK-NLP signalling network, we explored genome-wide transcriptional profiling in the nitrate-responsive transient transactivation system[12,17,18]. We discovered that NLP7-HA but not NLP7(S205A)-HA could robustly activate a wide range of putative NLP7 target genes in mesophyll cells (Extended Data Fig. 9a-c and Supplementary Table 1, 2)[1,12,17,18,32]. Notably, NLP7 could also target and ectopically activate *NRT2.1* and *TPPB*, which are normally silenced in mesophyll cells but are nitrate inducible in root cells (Fig. 3, Extended Data Fig. 9a, c). Our results are consistent with the activation of *NRT2.1-LUC*, *NRE-LUC* or *NIR-LUC* by ectopic NLP1,2,5,6,7,9 expression[17,18], the repression of primary nitrate responsive marker genes in dominant-negative NLP6 (NLP6-SUPRD) transgenic plants[12,17], as well as ChIP-chip analyses of NLP7-GFP after 10-min nitrate treatment in transgenic seedlings[18]. Interestingly, we also identified potential NLP7 target genes for cell cycle initiation and auxin hormone regulators (Extended Data Fig. 9b, c). Future research will aim

to fully elucidate the functions of specific NLP7 target genes in various plant organs and cell types. The identification of novel NLP7 target genes was supported by the unique *nlp7* phenotypes and the complementation of *nlp7* by NLP7-GFP but not NLP7(S205A)-GFP for proliferation and growth in shoots and roots (Fig. 6e, f and Extended Data Fig. 10). The broad spectrum of nitrate-associated mutant phenotypes and primary nitrate-responsive-transcriptome defects were shared by *icpk* and *nlp7*[14,18]. As the specific serine residue is conserved among *Arabidopsis* NLPs and LjNLPs (Extended Data Fig. 7e), CPK10/30/32 could potentially phosphorylate and activate all NLPs and possibly other TFs with overlapping or distinct target genes to support transcriptional, metabolic and system-wide nutrient-growth regulations differentially manifested in WT and conditional *icpk* mutant plants (Fig. 2g, 3–6 and Extended Data Fig. 3–10)[6,12,14,17,18,25].

Discussion

We have uncovered a nitrate-coupled Ca^{2+} signalling mechanism central to the plant nutrient-growth regulatory network using multifaceted approaches, encompassing an ultrasensitive Ca^{2+} biosensor, a sensitized and targeted functional genomic screen, a chemical switch for conditional higher-order *Arabidopsis cpk* mutants, as well as integrated cellular, biochemical, genetic and systems analyses. Our findings connected a novel Ca^{2+}-CPK-NLP signalling cascade to comprehensive nitrate responses and revealed a previously unrecognized function of Ca^{2+}-sensor CPKs as master regulators in orchestrating nitrate-activated signalling (Fig. 6g). As CPKs and NLPs are evolutionarily conserved from algae to land plants[12,14,17,18,28–30], the nitrate-CPK-NLP signalling relay may be widespread in the plant kingdom. Our discoveries expand the biological functions of Ca^{2+} signalling to nutrient responses essential to all life forms. Future research will likely identify new sensors, channels and other regulators involved in generating complex Ca^{2+} signatures in plant responses to nitrate, other nutrients, peptides, hormones, and environmental cues capitalizing on continued advances of ultrasensitive Ca^{2+} biosensors[36]. This work provides a molecular framework for future research on the complex interactions between glucose and nitrogen signalling pathways central to all aspects of nutrient-mediated growth regulation in plants and animals[1–8].

METHODS

Plasmid constructs and transgenic lines

The 1.3 kb GCaMP6 coding region was PCR amplified from the *pGP-CMV-GCaMP6s* plasmid (Addgene)[45]. The amplified DNA was then inserted into the plant expression vector (the *HBT-HA-NOS* plasmid)[46] to generate the *HBT-GCaMP6-HA* construct. The *HBT-GCaMP6-HA* construct was inserted into the binary vector *pCB302*[47] to generate the *HBT-GCaMP6-HA* transgenic plants using the *Agrobacterium* (GV3101)-mediated floral-dip method[48]. Transgenic plants were selected by spraying with the herbicide BASTA. The construct expressing *HY5-mCherry* used as a control for protoplast co-transfection and nucleus-labelling was obtained from Dr. Jin-Gui Chen[49]. *NLS-Td-Tomato* used as a control for protoplast co-transfection and nucleus-labelling was obtained from Dr. Xiayan Liu. *NIR-LUC* was constructed as described previously[16]. *UBQ10-GUS* that is a control for protoplast

co-transfection and internal control, all *HBT-CPKac-FLAG-NOS* expression plasmids have been described[27]. To construct *HBT-CPK-GFP-NOS*, the coding region of the *CPK10, 30, 32* cDNA was amplified and then cloned into the *HBT-GFP-NOS* plasmid[27]. *HBT-CPK10(M141G)-FLAG* was generated by site-directed mutagenesis of the *HBT-CPK10-FLAG* construct. To complement the *cpk10, 30/+* mutant, a 5.5 kb DNA fragment including the promoter region (3 kb) and the coding region of *CPK10* was amplified from genomic DNA, which was then cloned into the plasmid *HBT-HA-NOS* and mutagenized to generate *pCPK10-CPK10(M141G)-HA-NOS*. The *pCPK10-CPK10(M141G)-HA-NOS* construct was inserted into *pCB302* and transformed into *cpk10, 30/+* mutant plants using the *Agrobacterium* (GV3101)-mediated floral-dip method[48]. At the T3 generation, homozygous single copy insertion lines were screened for the *cpk10,30* double mutant carrying *pCPK10-CPK10(M141G)-HA-NOS* to obtain the 3MBiP-inducible *icpk10,30* double mutant, which rescued the embryo lethality of the *cpk10,30* double mutant. The 3MBiP-inducible *icpk10,30,32* triple mutant expressing CPK10(M141G)-HA (designated *icpk*) was generated by genetic cross to *cpk32* and confirmed by molecular analyses. To construct *35SΩ-NLP6-MYC* or *35SΩ-NLP7-MYC* in the *pCB302* binary plasmid with hygromycin B selection, the β-glucuronidase (GUS) gene in the *35SΩ-GUS* plasmid[50] was replaced with the DNA fragment encoding the full-length NLP6 or NLP7 fused to 6 copies of the MYC epitope tag in the *HBT-NLP6-MYC* or *HBT-NLP7-MYC* plasmid[17]. The *NLP6-MYC* and *NLP7-MYC* transgenic plants were generated by *Agrobacterium* (GV3101)-mediated transformation by floral dip and hygromycin B resistance selection. To construct *HBT-NLP7-HA* and *HBT-NLP7-GFP*, the 2.9 kb coding region of the *NLP7* cDNA was amplified and then cloned into the *HBT-NOS* plasmid. *HBT-NLP7(S205A)-HA* and *HBT-NLP7(S205A)-GFP* were generated by site-directed mutagenesis. A 7.9 kb genomic DNA fragment of *NLP7* was cloned into the *pUC* plasmid and fused with *GFP* at the C-terminus to generate *pNLP7-NLP7-GFP*. The *pNLP7-NLP7(S205A)-GFP* construct was generated by site-directed mutagenesis. *pNLP7-NLP7-GFP* or *pNLP7-NLP7(S205A)-GFP* was then inserted into *pCB302* and introduced into *nlp7–1* mutant plants using the *Agrobacterium* (GV3101)-mediated floral-dip[48] method for complementation analyses. To construct *UBQ10-CPK10KM-YN* and *UBQ10-NLP7-YC*, the coding regions of CPK10KM, NLP7, YFP-N terminus and YFP-C terminus were amplified by PCR and cloned into *UBQ10-GUS* plasmid. To construct *pET14-NLP7-N(1–581)-HIS* and *pET14-NLP7-N(S205A)-HIS* for protein expression, the N-terminal coding region of NLP7 and NLP7 S205A were amplified from *HBT-NLP7-HA* and *HBT-NLP7(S205A)-HA*. All constructs were verified by sequencing. The primers used for plasmid construction and site-directed mutagenesis are listed in Supplementary Table 3.

Plant materials and growth conditions

Arabidopsis ecotype Columbia (Col-0) was used as wild type (WT). The *cpk* mutants were obtained from Arabidopsis Biological Resource Centre (ABRC)[51]. Homozygous T-DNA lines were identified by using *CPK* gene specific primers and T-DNA left border primers. The gene specific primers used are listed in the Supplementary Table 4. Double mutants were obtained by genetic crosses between *cpk10–1, cpk30–1 and cpk32–1*, and confirmed by PCR. For RT-PCR analysis of *cpk* single mutants, around 30 plants were grown on the petri dish (150 mm × 15 mm) containing 100 ml of ½× MS medium salt, 0.1% MES, 0.5%

sucrose, 0.7% phytoagar under constant light (150 μmol/m²s) at 23°C for 7 days. Samples were collected for RT-PCR analysis. To generate *icpk*, *cpk32–1* was crossed to *icpk10,30*. F2 plants were first screened for resistance to BASTA and then confirmed by genotyping (primers listed in Supplementary Table 4) for the homozygous *cpk10,30,32* triple mutants. The homozygous *icpk* plants were isolated with no segregation for BASTA resistance in F3 plants. For demonstrating the embryo lethality in *cpk10,30*, *cpk10, cpk30/+* plants were grown under 16/8 h photoperiod (100 μmol/m²s) at 23/20°C. Siliques were opened using forceps and needles under a dissecting microscope (Leica MZ 16F). Images were acquired and processed using IM software and Adobe Photoshop (Adobe). For obtaining nitrate-free mesophyll protoplasts, around 16 to 20 plants were grown on the petri dish (150 mm × 15 mm) containing 100 ml of nitrogen-free 1× MS medium salt, 0.1% MES, 1% sucrose, 0.7% phytoagar, 2.5 mM ammonium succinate and 0.5 mM glutamine, pH 6 under 12/12 h photoperiod (75 μmol/m²s) at 23/20°C for 23–28 days. Mesophyll protoplasts were isolated from the second and the third pair of true leaves following the mesophyll protoplast isolation protocol[47]. For monitoring plant growth without exogenous nitrogen source after germination, thirty seedlings were germinated and grown on a basal medium[16] (10 mM KH_2PO_4/KH_2PO_4, 1 mM $MgSO_4$, 1 mM $CaCl_2$, 0.1 mM $FeSO_4$-EDTA, 50 μM H_3BO_4, 12 μM $MnSO_4·H_2O$, 1 μM $ZnCl_2$, 1 μM $CuSO_4·5H_2O$, 0.2 μM $Na_2MoO_4·2H_2O$, 0.1% MES and 0.5% sucrose, pH 5.8) with 1 % phytoagar under constant light (150 μmol/m²s) at 23°C for four days. Photos were taken at different days (Day 1 to 4) using a dissecting microscope (Leica MZ 16F) with IM software. For analysing the specific plant growth programs in response to different exogenous nitrogen sources at different concentrations, seedlings were germinated and grown on a basal medium for 4 days as described above, and then transferred to the basal medium with 0.1, 0.5, 1, 5 or 10 mM KNO_3, NH_4Cl, glutamine or KCl for additional 1 to 7 days. For gene expression analyses with RT-qPCR and RNA-Seq, 10 seedlings were germinated in one well of the 6-well tissue culture plate (Falcon) with 1 ml of the basal medium supplemented with 2.5 mM ammonium succinate as the sole nitrogen source. Plates were sealed with parafilm and placed on the shaker at 70 rpm under constant light (45 μmol/m²s) at 23°C for 7 days. Before nitrate induction, seedlings were washed three times with 1 ml basal medium. Seedlings were treated in 1 ml of the basal medium with KCl or KNO_3 for 15 min. Seedlings were then harvested for RNA extraction with TRIzol (Thermo Fisher Scientific). For blocking the kinase activity of CPK10(M141G), seedlings were pre-treated with 10 μM 3MBiP in the basal medium for 2 min and then treated with KCl or KNO_3 for 15 min. For the assays with Ca^{2+} channel blockers and Ca^{2+} sensor inhibitors, seedlings were pre-treated with 2 mM $LaCl_3$, 2 mM $GdCl_3$, 250 μM W5, or 250 μM W7 in the 1 ml of the basal medium for 20 min, and then induced by 0.5 mM KCl or KNO_3 for 15 min. For monitoring root morphology, seedlings were germinated and grown on a basal medium supplemented with 2.5 mM ammonium succinate and 1% phytoagar under constant light (150 μmol/m²s) at 23°C for 3 days. Plants were then transferred to the basal medium supplemented with 1 μM 3MBiP and 5 mM KNO_3, 2.5 mM ammonium succinate, 5 mM KCl or 1 mM glutamine and grown for 5 to 8 days. After seedling transfer, 1 ml of 1 μM 3MBiP was added on the medium every two days. For monitoring lateral root developmental stages, seedlings were monitored under a microscope (Leica DM5000B) with a 20× objective lens according to the protocol as described previously[44]. In order to measure the primary and lateral root length, pictures were taken

using a dissecting microscope (Leica MZ 16 F) with IM software and analysed by ImageJ. For comparing the shoot phenotype, 8-day-old seedlings were cut above the root-shoot junction for measuring the shoot fresh weight and acquiring images. To analyse the *cpk* single mutant phenotype, plants were germinated and grown on the ammonium succinate medium for 3 days and then transferred to basal medium plates supplemented with 5 mM KNO_3 for 6 days. For analysing double mutants in response to 3MBiP, plants were transferred to basal medium plate supplemented with 5 mM KNO_3 and 1 μM 3MBiP for 6 days, and 3MBiP was reapplied every 2 days. Individual 9-day-old seedling (n=12) was collected for measuring fresh weight and acquiring images. For characterizing the shoot phenotype of *nlp7-1* and the complementation lines, around 20 seeds were germinated on the petri dish (150 mm × 15 mm) containing 100 ml of nitrogen-free 1× MS medium salt (Caisson), 0.1% MES, 1% sucrose, 0.7% phytoagar and 25 mM KNO_3 medium pH 5.8 under 16/8 h photoperiod (100 μmol/m^{2}s) at 18°C and grown for 21 days. The shoots were collected for measurement of fresh weight and acquisition of images. For analyses of the shoot phenotype in *icpk*, seeds were germinated and grown on the ammonium succinate basal medium plate for 3 days and then transferred to the same medium supplemented with 1 μM 3MBiP. The inhibitor 3MBiP (5 ml of 1 μM) was reapplied on the medium two more times during the growth.

Aequorin reconstitution and bioluminescence-based quantification of Ca^{2+} signals in whole seedlings

Two transgenic seedlings expressing apoaequorin[26] were germinated and grown in one well of a 12-well tissue culture plate (Falcon) with 0.5 ml of the basal medium supplemented with 2.5 mM ammonium succinate for 6 days. Individual plant was transferred to a luminometer cuvette filled with 100 μl of the reconstitution buffer (2 mM MES pH 5.7, 10 mM $CaCl_2$, and 10 μM native coelenterazine from NanoLight Technology) and incubated at room temperature in dark overnight. The emission of photons was detected every sec using the luminometer BD Monolight™ 3010. Injection of 100 μl of 20 mM KCl, 20 mM KNO_3, 200 nM flg22 or ultrapure water into the cuvettes initiated the measurement. Luminescence values were exported and processed using Microsoft Excel software.

GCaMP6-based Ca^{2+} imaging in mesophyll protoplasts and transgenic seedlings

For Ca^{2+} imaging in protoplasts, mesophyll protoplasts (2×10^5) in 1 ml buffer were co-transfected with 70 μg of *HBT-GCaMP6* and 50 μg of *HBT-HY5-mCherry* plasmid DNA. Transfected protoplasts were incubated in 5 ml of WI buffer[46] for 4 h. Before time-lapse recording, a cover glass was placed on a 10-well chamber slide covering ¾ part of a well, and placed on the microscope stage. Mesophyll protoplasts co-expressing GCaMP6 and HY5-mCherry (2×10^4 protoplast cells) were spun down for 1 min at 100×g. WI-Ca^{2+} buffer (WI buffer with 4 mM $CaCl_2$) (0.5 μl) with different stimuli (40 mM KCl, 40 mM KNO_3, or 40 mM NH_4Cl) or 80 mM Ca^{2+} chelator (EGTA) were added into 1.5 μl of concentrated mesophyll protoplasts in WI buffer. The final concentration of each stimulus was 10 mM KCl, 10 mM KNO_3, 10 mM NH_4Cl or 20 mM EGTA in the solution. The stimulated protoplasts were immediately loaded onto the slide and imaged via the Leica AF software on a Leica DM5000B microscope with the 20× objective lens. The exposure time for GCaMP6 was set at 1 sec and recorded every 2 sec to generate 199 frames. The exposure

time was set at 45 millisecond for the bright field and 1 sec for the mCherry signal. The fluorescence intensity was determined with the region of interest (ROI) function for each protoplast. The intensity data were exported and processed using Microsoft Excel software. The images were exported and processed using Adobe Photoshop software. To make a video, individual images were cropped using Adobe Photoshop software and saved in JPEG format. The video was generated using ImageJ with the cropped images. For Ca^{2+} imaging with the *GCaMP6* transgenic seedling cotyledons, 5 seedlings were germinated in one well of a 6-well tissue culture plate (Falcon) with 1 ml of the basal medium supplemented with 2.5 mM ammonium succinate for 7 days. A chamber was made on microscope slides between two strips of the invisible tape (0.5 cm × 3 cm) and filled with 150 μl of the basal medium. A cotyledon of the 7-day-old seedling was cut in half using razor blade and embedded in the medium. A thin layer of cotton was placed on top of the cotyledon to prevent moving. The coverslip was placed on the sample and fixed by another two strips of the invisible tape. The cotyledon was allowed to recover on the slide for 10 min. Confocal imaging was acquired using the Leica laser scanning confocal system (Leica TCS NT confocal microscope, SP1). The mesophyll cells in the cotyledon were targeted for Ca^{2+} imaging at the focal point. Basal medium (200 μl) with 10 mM KCl, 10 mM KNO_3 or 20 mM EGTA was loaded along one edge of the coverslip. A Kimwipes tissue on the opposite edge was used to draw the buffer into the chamber. To record fluorescence images, the excitation was provided at 488 nm and emission images at 515–550 nm were collected. The scanning resolution was set at 1,024 × 1,024 pixels. Images were captured every 10 sec and averaged from two frames. Eighty images total were collected and processed using Adobe Photoshop software. A video was generated with collected images using the method described above. For Ca^{2+} imaging with the *GCaMP6* transgenic seedling at the root tip and the elongated region of roots (around the middle region of the root), ten seedlings were germinated and grown on the tissue culture plate (Falcon) with the basal medium and 1% phytoagar under constant light (150 μmol/m^{2}s) at 23°C for 4 days. The images were obtained using Leica laser scanning confocal system as described above for cotyledon Ca^{2+} imaging. Thirty three images were collected and processed using Adobe Photoshop software. A video was generated with collected images using the method described above.

Mesophyll protoplast transient expression assays

Time-course, specificity and dosage analyses of *NIR-LUC* activity in response to nitrate induction was carried out in mesophyll protoplasts (2×10^4 protoplasts in 100 μl) co-transfected with 10 μg *NIR-LUC* and 2 μg *UBQ10-GUS* (as the internal control) and incubated in WI buffer[46] for 4 h, and then induced by 0.5 mM KCl, KNO_3, NH_4^+ or Gln or different concentrations of KNO_3 for 2 h. For time-course analysis, the fold change is calculated relative to the value of KCl treatment at each time point. For nitrate-sensitized functional genomic screen, nitrate-free mesophyll protoplasts (2×10^4 protoplasts in 100 μl) were co-transfected with 8 μg of *HBT-CPKac* (constitutively active CPK) or a control vector, 10 μg of *NIR-LUC* and 2 μg of *UBQ10-GUS* plasmid DNA, and incubated for 4 h to allow CPKac protein expression. For investigating the functional relationship between CPKac10 and NLP7 in nitrate signalling, nitrate-free mesophyll protoplasts (4×10^4 protoplasts in 200 μl) were co-transfected with 8 μg of *NIR-LUC* and 2 μg of *UBQ10-GUS* plasmid DNA as well as 5 μg of *HBT-CPKac10, or HBT-CPKac10KM* or a control vector or

HBT-NLP7 or *HBT-NLP7*(*S205A*) in different combinations supplemented with 5 μg control vector to reach a total 20 μg per transfection reaction, and incubated for 4 h for protein expression. Protoplasts were then induced with 0.5 mM KCl or KNO$_3$ for 2 h. The luciferase assay and GUS assay were carried out as described before[46]. The expression levels of NLP7-HA and CPK-FLAG/CPK10ac-FLAG in protoplasts were monitored by immunoblot with anti-HA-peroxidase (Roche, #11667475001) (1:2000) and anti-FLAG-HRP (Sigma, A8592) (1:2000) antibodies, respectively.

Protein expression and purification—Expression vectors were transformed into Rosetta™ 2 (DE3) pLysS Competent Cells (Novagen). Cells were induced by 1 mM of IPTG when OD600 reached 0.6, and proteins were expressed at 18°C for 18 h. Affinity purification was carried out using HisTrap columns (GE Healthcare) and ÄKTA FPLC system. Purified proteins were buffer exchanged into PBS using PD-10 Desalting Columns (GE Healthcare), and then concentrated by Amicon Ultra-4 Centrifugal Filter Unit with Ultracel-10 membrane (EMD Millipore).

In-gel protein kinase assay

Around 10^6 protoplasts were incubated in WI buffer (5 ml) in petri dishes (9 × 9 cm) for 4 h before induction with 10 mM KCl or KNO$_3$ for 10 min. Protoplasts were harvested and lysed in 200 μl of extraction buffer: 150 mM NaCl, 50 mM Tris-HCl pH 7.5, 5 mM EDTA, 1% Triton X-100, 1× protease inhibitor cocktail (Complete mini, Roche) and 1 mM DTT. The protein extract supernatant was obtained after centrifugation at 14,000 rpm for 10 min at 4°C. Total proteins (20 μg) were loaded on 8% SDS-PAGE embedded with or without 0.5 mg/ml histone type III-S (Sigma) as a general CPK phosphorylation substrate[27]. The gel was washed 3 times with the washing buffer (25 mM Tris-HCl pH7.5, 0.5 mM DTT, 5 mM NaF, 0.1 mM Na$_3$VO$_4$, 0.5 mg/ml BSA and 0.1% Triton X-100), and incubated for 20 h with three changes in the renaturation buffer (25 mM Tris-HCl pH7.5, 0.5 mM DTT, 5 mM NaF and 0.1 mM Na$_3$VO$_4$) at 4°C. The gel was then incubated in the reaction buffer (25 mM Tris-HCl pH 7.5, 2 mM EDTA, 12 mM MgCl$_2$, 1 mM CaCl$_2$, 1 mM MnCl$_2$, 1 mM DTT and 0.1 mM Na$_3$VO$_4$) with or without 20 mM EGTA at room temperature for 30 min. The kinase reaction was performed for 1 h in the reaction buffer supplemented with 25 μM cold ATP and 50 μCi [γ-^{32}P]ATP with or without 20 mM EGTA. The reaction was stopped by extensive washes in the washing buffer (5% trichloroacetic acid and 1% sodium pyrophosphate) for 6 h. The protein kinase activity was detected on the dried gel using the Typhoon imaging system (GE Healthcare).

1-Isopropyl-3-(3-methylbenzyl)-1*H*-pyrazolo[3,4-*d*]pyrimidin-4-amine (3MBiP) synthesis

3MBiP was synthesized using the same procedures as those for a close structural analog, 3MB-PP1[42], with comparable yields, except that *iso*-propylhydrazine was substituted for *tert*-butylhydrazine.

^{1}H NMR (400 MHz, DMSO-*d$_6$*) δ 8.12 (s, 1H), 7.15 (d, *J* = 7.6 Hz, 1H), 7.08 (s, 1H), 7.00 (t, *J* = 7.5 Hz, 2H), 4.96 (p, *J* = 6.7 Hz, I H), 4.31 (s, 2H), 2.24 (s, 3H), 1.44 (d, *J* = 6.7 Hz, 6H). ^{13}C NMR (100 MHz, DMSO-*d$_6$*) δ 158.41, 155.78, 153.69, 143.12, 139.56, 137.85,

129.51, 128.79, 127.30, 125.87, 98.92, 48.18, 40.10, 33.70, 22.23, 21.54. ESI-MS calculated for $C_{16}H_{20}N_5$ [M+H]$^+$ is 282.2, found 282.7.

In vitro protein kinase assays

For *in vitro* kinase assay with CPK10(M141G)-FLAG or CPK10-FLAG, 4×10^4 protoplasts expressing CPK10(M141G)-FLAG or CPK10-FLAG were lysed in 200 μl immunoprecipitation (IP) buffer that contained 50 mM Tris-HCl pH7.5, 150 mM NaCl, 5 mM EDTA, 1 mM DTT, 2 mM NaF, 2 mM Na$_3$VO$_4$, 1 % TritonX-100 and 1× protease inhibitor cocktail (Complete mini, Roche). Protein extracts were incubated with 0.5 μg anti-FLAG antibody (Sigma, #F1804) at 4°C for 2 h and additional 1 h with protein G Sepharose beads (GE Healthcare). The immunoprecipitated kinase protein was washed three times with IP buffer and once with kinase buffer (20 mM Tris-HCl pH 7.5, 15 mM MgCl$_2$, 1 mM CaCl$_2$ and 1 mM DTT). Kinase reactions were performed for 1 h in 25 μl kinase buffer containing 1 μg of histone (Sigma #H5505 or H4524), 50 μM cold ATP and 2 μCi [γ-^{32}P]ATP. To block the CPK10(M141G)-FLAG kinase activity, 1 μM 3MBiP or DMSO as control was added in the 25 μl kinase buffer for 2 min before performing the kinase reaction. The reaction was stopped by adding SDS-PAGE loading buffer. After separation on a 12% SDS-PAGE gel, the protein kinase activity was detected on the dried gel using the Typhoon imaging system. For performing *in vitro* kinase assay with CPK10(M141G)-HA isolated from *icpk10,30* seedlings, twelve 7-day-old seedlings grown in 2 wells of a 6-well-plate with 1 ml medium (0.5× MS, 0.5% sucrose and 0.1% MES pH 5.7) were grounded in liquid nitrogen into powder and lysed in 200 μl of IP buffer. The CPK10(M141G)-HA protein was immunoprecipitated with the anti-HA antibody (Roche, #11666606001) and protein G Sepharose beads. *In vitro* kinase assay with CPK10(M141G)-HA proteins was carried out as described above. For *in vitro* kinase assay with the subgroup III CPKs, FLAG-tagged CPK7, 8, 10, 10 KM (K92M, a kinase-dead mutation in the conserved ATP binding domain), 13, 30, and 32 were expressed in 10^5 protoplasts and purified with 1 μg anti-FLAG antibody conjugated to protein G Sepharose beads as described above. CPK11-FLAG from subgroup I was used as a negative control to demonstrate the specificity of NLP7 as a substrate only for subgroup III CPKs. NLP7-HIS (~1 μg) purified from *E. coli* or Histone type III-S (2 μg) was used as substrate in the *in vitro* kinase assay. Kinase reactions were performed for 1 h at 28°C in 25 μl kinase buffer containing 5 μM cold ATP and 6 μCi [γ-^{32}P]ATP, which greatly enhanced the CPK activity. To reduce the background caused by free [γ-^{32}P]ATP in the gel, 50 μM cold ATP was added in the kinase reaction before sample loading in 10% (NLP7-HIS) or 12% (HIS) SDS-PAGE gel. To demonstrate that CPK10, 30, 32 kinase activities were Ca^{2+} dependent, 4×10^4 (CPK10 or CPK10ac) or 10^5 (CPK30, 32 or CPKac 30, 32) protoplasts expressing CPKs for 12 h instead of 6 h (to increase the yield of CPK proteins) were lysed in 200 μl (CPK10) or 400 μl (CPK30 or CPK32) of IP buffer. The CPK proteins were immunoprecipitated with anti-FLAG antibody (0.5 μg for CPK10 or CPKac10, and 2 μg for CPK30, 32 or CPKac 30, 32) conjugated to protein G Sepharose beads. The immunoprecipitated CPKs were washed three times with IP buffer and twice with EGTA-kinase buffer (20 mM Tris-HCl pH 7.5, 15 mM MgCl$_2$, 15 mM EGTA and 1 mM DTT). Kinase reactions were performed for 1 h at 28°C in 25 μl kinase buffer or EGTA-kinase buffer containing 5 μM cold ATP and 6 μCi [γ-^{32}P]ATP and purified NLP7-HIS (~1 μg), NLP7-N (1-581 a.a.) (~0.8 μg), NLP7-N(S205A) (~0.8 μg), or Histone type III-S (2 μg).

After performing kinase reaction, 50 μM cold ATP was added to reduce the background caused by free [γ-^{32}P]ATP. The reaction was stopped by adding SDS-PAGE loading buffer. After separation on a 12% SDS-PAGE gel (Histone type III-S) or 10% (NLP7-HIS or NLP7-N-HIS) SDS-PAGE gel, the protein kinase activity was detected on the dried gel using the Typhoon imaging system. Substrate was stained with InstantBlue Protein Stain (C.B.S. Scientific). The expression levels of CPK or CPKac proteins were monitored by immunoblot with anti-FLAG-HRP (Sigma, A8592) (1:4000) antibody. CPKac proteins without the Ca^{2+}-binding EF-hand domains provided constitutive kinase activities that were insensitive to EGTA. The sensitivity of CPK10, CPK30 and CPK32 to EGTA in kinase assays demonstrated their functions as Ca^{2+} sensors in nitrate signalling, which was further supported by the lack of NLP7-HA phosphorylation and the nuclear retention of NLP7-GFP in *icpk* mutant cells. Importantly, NLP7(S205A) lost nitrate-induced phosphorylation, nuclear localization, *NIR-LUC* activation, and endogenous target gene activation in WT protoplasts and seedlings.

RNA isolation, RT-PCR and RT-qPCR

RNA isolation, RT-PCR and RT-qPCR were carried out as described previously[16]. The primers used for RT-PCR and RT-qPCR are listed in Supplementary Table 5. The *TUBULIN 4* (*TUB4*) was used as a control in wild type and *cpk* mutants. The relative gene expression was normalized to the expression of *UBQ10*. Triplicate biological samples were analysed with consistent results.

RNA-Seq analyses

We chose the early time point to minimize secondary target genes and the complexity that negative feedback would have introduced, including indirect effects from assimilation of nitrate and the subsequent activation of transcriptional repressors[1,4,12,13,15,18]. Seven-day-old seedlings of wild type and *icpk* were pretreated with 10 μM 3MBiP for 2 min and then treated for 15 min with either 10 mM KCl or 10 mM KNO$_3$. Total RNA (0.5 μg) was used for preparing the library with the Illumina TruSeq RNA sample Prep Kit v2 according to the manufacture's guidelines with 9 different barcodes (triplicate biological samples). The libraries were sequenced for 50 cycles on an Illumina HiSeq 2500 rapid mode using two lanes of a flow cell. The sequencing was performed at MGH Next Generation Sequencing Core facility (Boston, USA). Fastq files, downloaded from the core facility, were used for data analysis. The quality of each sequencing library was assessed by examining fastq files with FastQC. Reads in the fastq file were first aligned to the *Arabidopsis* genome, TAIR10, using Tophat[52]. HTSeq[53] was used to determine the reads per gene. Finally, DESeq2[54] analysis was performed to determine differential expression[55]. For HTSeq normalized counts in each sample, differentially expressed genes were determined for WT KNO$_3$ vs. WT KCl and *icpk* KNO$_3$ vs. WT KNO$_3$. The differential expression analysis in DESeq2 uses a generalized linear model of the form

$$K_{ij} \sim NB(\mu_{ij}, a_i)$$

$$\mu_{ij} = s_{ij} q_{ij}$$

$$log_2(q_{ij}) = xj.\beta i$$

where counts K_{ij} for gene i, sample j are modeled using a Negative Binomial distribution with fitted mean μ_{ij} and a gene-specific dispersion parameter α_i. The fitted mean is composed of a sample-specific size factor s_j and a parameter q_{ij} proportional to the expected true concentration of fragments for sample j. The coefficients βi give the log2 fold changes for gene i for each column of the model matrix X. Results were imported into Microsoft Excel for filtering. In order to generate a list to minimize false positives of primary nitrate responsive genes in WT, we applied a relatively high stringency, q-value 0.05 cut-off, followed by a log_2 -1 or 1 cut-off.

To generate a heatmap, we performed agglomerative hierarchical clustering on genes with Gene Cluster 3.0[56] using Correlation (uncentered) as the similarity metric and single linkage as the clustering method. Java Treeview[57] was used to visualize the results of the clustering. To obtain a list of enriched gene functions, we used the Classification SuperViewer Tool on the BAR website (http://bar.utoronto.ca/ntools/cgi-bin/ntools_classification_superviewer.cgi) with the MapMan classification source option. Analyses of enriched functional categories with nitrate up-regulated and down-regulated genes were performed using the MapMan classification source option on the Classification SuperViewer Tool with manual annotation based on literature. The fold enrichment is calculated as follows: (Number in Class$_{input\_set}$/ Number of total$_{input\_set}$)/ (Number in Class$_{reference\_set}$/ Number of total$_{reference\_set}$). The p-value is calculated in Excel using a hypergeometric distribution test. The data in Extended Data Fig. 4c and 4d were sorted by fold enrichment with a p-value < 0.05 cutoff. For the biological duplicate RNA-Seq experiments for identifying NLP7 target genes in the mesophyll protoplast transient expression system, 500 μg of *HBT-NLP7-HA*, *HBT-NLP7(S205A)-HA* or control plasmid DNA was transfected into 10^6 protoplasts and incubated for 4.5 h. Total RNA (0.5 μg) was used to construct the libraries with 6 different barcodes (biological duplicate samples) as described above. The sequencing result was performed and analysed as described above. Differentially expressed genes were determined with DESeq2 on NLP7 vs. Ctl (Control) and NLP7(S205A) vs. Ctl. Results were imported into Microsoft Excel for filtering (log_2 1 cut-off) and generating heatmaps.

Immunoblot analyses of nitrate-induced phosphorylation of NLP6 and NLP7 *in vivo*

Transgenic seedlings expressing NLP6-MYC or NLP7-MYC were germinated and grown in basal medium containing 0.5 mM ammonium succinate as a sole nitrogen source (0.01% MES-KOH, pH 5.7) for 4 days at 23°C under continuous light (60 μmol/m^{2}s). After replacement with fresh medium supplemented with 10 mM KCl or KNO$_3$, the seedlings were collected after incubation for 5, 10 or 30 min. For examining the effects of Ca^{2+} channel blockers and Ca^{2+} sensors inhibitors, the 4 day-old seedlings were placed in fresh basal medium supplemented with 2 mM LaCl$_3$, 2 mM GdCl$_3$, 250 μM W5 or 250 μM W7 for 20 min and induced by 10 mM KCl or KNO$_3$. The seedlings were weighed, frozen in

liquid nitrogen and ground using a Multibeads Shocker (Yasui Kikai, Osaka, Japan). The ground samples were suspended in 20 volume of 1× Laemmli sample buffer supplemented with twice the concentration of EDTA-free Protease Inhibitor Cocktail (Roche) and heated at 95°C for 30 sec. Samples were then spun down and the supernatant was subjected to SDS-PAGE and immunoblotting with anti-MYC (Millipore, #05-419) (1:1000) and anti-Histone H3 (Abcam, #ab1791) (1:5000) antibodies. For calf intestinal alkaline phosphatase (CIP) treatment, proteins in 1.2-fold CIP buffer (60 mM Tris-HCl pH8.0, 120 mM NaCl, 12 mM MgCl$_2$, 1.2 mM DTT, 2.4-fold concentration of EDTA-free Protease Inhibitor Cocktail) were mixed with CIP solution (New England Biolabs, M0290, 10 U/µl) in a ratio of 5 (CIP buffer): 1 (CIP solution) and incubated at 37°C for 30 min. For a control treatment, heat-inactivated CIP was mixed. The reactions were stopped by adding an equal volume of 2× Laemmli sample buffer and heating at 95°C for 30 sec. To demonstrate that nitrate-induced NLP7 phosphorylation was abolished in *icpk* by protein mobility shift in SDS-PAGE, 4 × 10^4 protoplasts isolated from wild type or *icpk* were transfected with 20 µg of NLP7-HA or NLP7-S205A-HA. To block CPK10(M141G) activity in *icpk*, 10 µM 3MBiP was added in the incubation buffer (WI) after transfection. After expressing protein for 4.5 h, protoplasts were then induced by 10 mM KCl or KNO$_3$ for 15 min. Protoplasts were spun down and re-suspended in 40 µl 1× Laemmli sample buffer. Samples (10 µl) were separated in a 6% SDS-PAGE resolving gel without a stacking gel layer. After transferring proteins to the PVDF membrane, the NLP7 (WT and S205A) proteins were detected with anti-HA-peroxidase (Roche, #11667475001) (1:2000). RuBisCo was detected by an anti-Rubisco antibody (Sigma, GW23153) (1:5000) as a loading control.

Detection of the serine 205 phosphorylation in NLP7 *in vivo*

Transformation of T87 cell suspension culture derived from a seedling of *Arabidopsis thaliana* L. (Heynh.) ecotype Columbia[58] was conducted with the *35SΩ-NLP7-MYC* construct in the *pCB302* binary plasmid carrying the hygromycin B selection marker gene. Transformants mediated by *Agrobacterium* (GV3101) were selected on agar plates (JPL medium, 3 g/L gellun gum, 500 mg/L carbenicillin and 20 mg/L hygromycin), and the transformants were maintained in liquid JPL medium as described previously[58]. T87 cells expressing NLP7-MYC were incubated in nitrogen free-JPL liquid medium for 2 days, and then 10 mM KNO$_3$ was added into the medium. After 30 min treatment, the T87 cells (approximately 4 g F.W.) were frozen in liquid nitrogen and homogenized with Multi-beads Shocker (Yasui Kikai, Osaka, Japan) in 10 mL of the buffer that contained 25 mM Tris-HCl pH 7.5, 150 mM NaCl, 0.1% NP-40, 10% glycerol, 1× Complete Protease Inhibitor Cocktail and 1× PhosSTOP (Roche). Cell lysates obtained were incubated with anti-MYC antibodies crosslinked to Dynabeads (Invitrogen). Trapped proteins were eluted by 1× Laemmli sample buffer and separated by SDS-PAGE. Gel pieces containing NLP7-MYC were recovered and subjected to *in-gel* double digestion with trypsin (10 ng/µl) and chymotrypsin (10 ng/µl) (Promega, Madison, WI). NanoLC-ESI-MS/MS analysis was performed as described previously[59,60] with minor modifications.

NLP7, CPK10, CPK30, and CPK32 nuclear localization analyses

For analysing NLP7 nuclear retention triggered by nitrate in protoplasts, nitrate-free mesophyll protoplasts (4 × 10^4 protoplasts in 200 µl) were co-transfected with 20 µg of

NLP7-GFP or NLP7(S205A)-GFP and 10 μg of *HBT-HY5-mCherry* plasmid DNA and incubated for 6 h. Mesophyll protoplasts were spun down for 1 min at 100×g. WI buffer with 10 mM KCl or KNO_3 was added into mesophyll protoplasts for 30 min. The treated protoplasts were loaded onto slides and imaged with the 20× objective lens on a Leica DM5000B microscope operated with the Leica AF software. The images were collected and processed using Adobe Photoshop software. For analysing NLP7-GFP nuclear retention triggered by nitrate in transgenic lines, NLP7-GFP/*nlp7-1* and NLP7(S205A)-GFP/*nlp7-1* seedlings were germinated and grown on the basal medium supplemented with 2.5 mM ammonium succinate and with 1 % phytoagar under constant light (150 μmol/m^{2}s) at 23°C for 5 days. Plants were placed on the slide as described above and stimulated by 10 mM KNO_3. Confocal images were acquired as described for GCaMP6-based Ca^{2+} imaging in transgenic seedlings. For analysing CPK10, CPK30 and CPK32 nuclear localization in response to nitrate, nitrate-free mesophyll protoplasts (4×10^4 protoplasts in 200 μl) were co-transfected with 20 μg of *CPK10-GFP* or *CPK30-GFP* or *CPK32-GFP* and 10 μg of *HBT-HY5-mCherry* plasmid DNA and incubated for 12 h. Protoplasts were then treated with 10 mM KNO_3 for 5 min. Confocal imaging was acquired using the Leica Application Suite X software on a Leica TCS SP8 (Leica) confocal microscope with the 40× objective lens. To obtain fluorescence images, the excitation was set at 489 nm (GFP) and 587 nm (mCherry), and emission images at 508 nm (GFP) and 610 nm (mCherry) were collected. The scanning resolution was set at $1,024 \times 1,024$ pixels. The images were collected and processed using Adobe Photoshop software. For analysing NLP7-GFP nuclear retention in wild type and *icpk*, nitrate-free mesophyll protoplasts (4×10^4 protoplasts in 200 μl) were co-transfected with 20 μg of *NLP7-GFP* and 4 μg of *HBT-Td-Tomato* plasmid DNA and incubated for 12-16 h. The transfected protoplasts were treated with inhibitor 10 μM 3MBiP 30 min before nitrate induction. Protoplasts were treated with 10 mM KNO_3 for 15 min in the presence of 10 μM 3MBiP of WI buffer. The images were acquired as described above for the NLP7 nuclear retention in protoplasts.

BiFC assay

Nitrate-free mesophyll protoplasts (4×10^4 protoplasts in 200 μl) were co-transfected with 18 μg of *UBQ10-CPK10KM-YN*, *UBQ10-NLP7-YC*, and 4 μg of *HBT-HY5-mCherry* plasmid DNA, and incubated for 12-18 h. Protoplasts were then treated with 10 mM KNO_3 for 2 h. Confocal images were acquired as described above for CPK localization in response to nitrate.

Statistical analysis

The chosen sample sizes for all experiments were empirically determined by measuring the mean and standard deviation for the sample population in pilot experiments, and then calculated (the 1-Sample Z-test method, two-sided test) with the aim to obtain the expected mean of less than 25% significant difference with the alpha value 0.05 and the power of the test 0.80. For multiple comparisons, data were first subjected to one-way or two-way ANOVA, followed by Tukey's multiple comparisons test to determine statistical significance. To compare two groups, Student's t-test was used instead. To compare WT and *icpk* lateral root development, data were categorized into two groups, and then subjected to Chi-square test, as indicated in the figure legends.

Data Availability
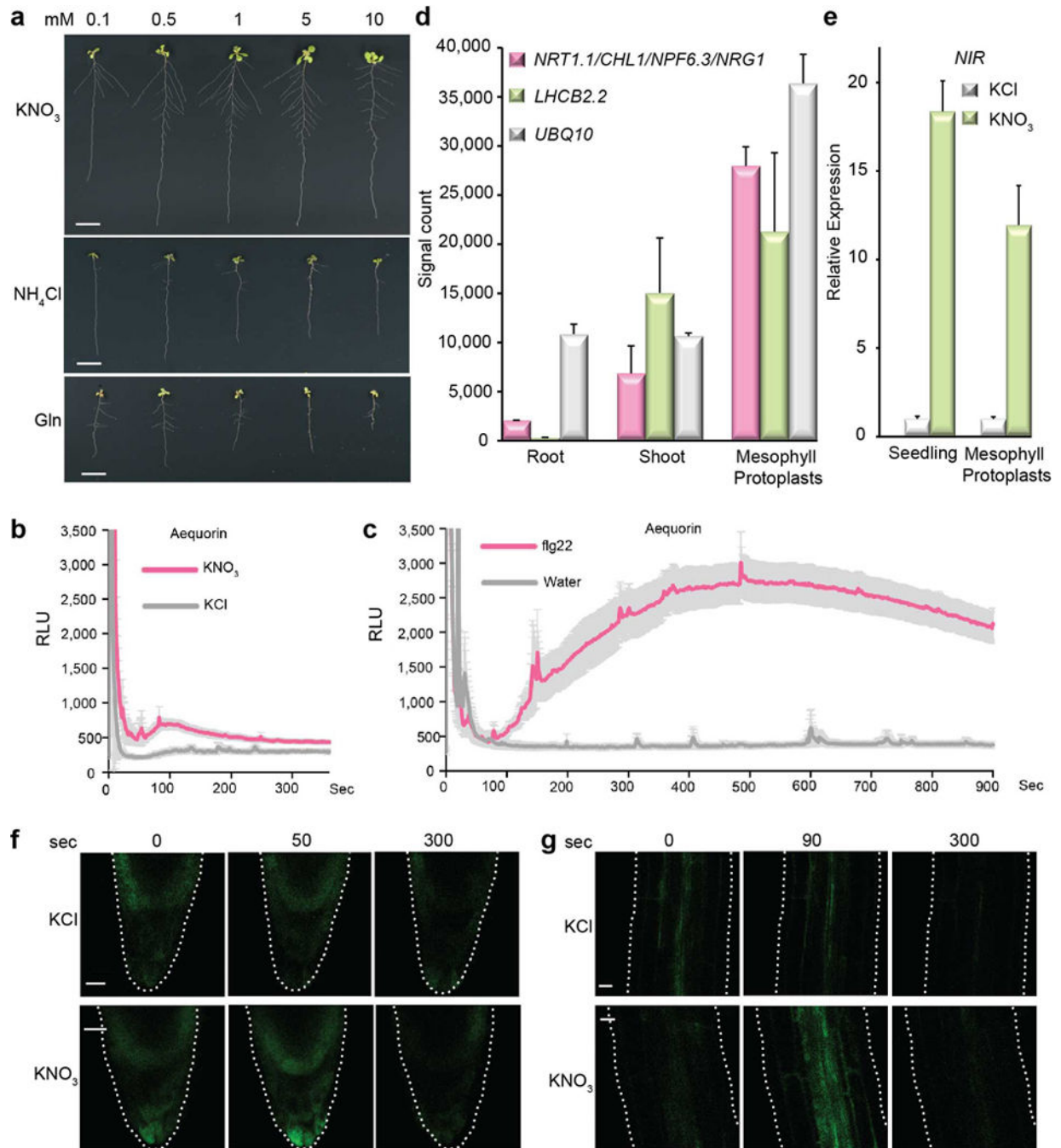
Extended Data

Extended Data Figure 1. Nitrate promotes plant development and induces Ca²⁺ signatures in both leaves and roots

a, Nitrate promotes both shoot and root development. Plants were germinated without exogenous nitrogen source for 4 days and then transferred to the plates supplemented with different concentrations of KNO_3, NH_4Cl or glutamine (Gln) for 7 days. Scale bar, 1 cm. The experiments were repeated twice with 10 seedlings for each treatment with consistent results. **b**, **c**, Distinct Ca^{2+} signatures induced by nitrate and flg22 in aequorin transgenic plants. *Arabidopsis* transgenic seedlings constitutively expressing the Ca^{2+} reporter protein apoaequorin were grown in liquid medium containing 2.5 mM ammonium succinate as the sole nitrogen source for 6 days. Aequorin was reconstituted with 10 μM coelenterazine for overnight in the dark. The results are presented as relative light units (RLU) in response to 10 mM KCl or KNO_3 (**b**) or in response to 100 nM flg22 or water (**c**) at intervals of 1 sec. Error bars, ±s.e.m, n=10 seedlings. The experiments were repeated three times with similar results. The RLU value is cut off at 3,500. **d**, *NRT1.1/CHL1/NPF6.3/NRG1* is highly expressed in shoots and mesophyll protoplasts. The signal counts of the genes in roots and shoots were derived from previously published microarray data[1]. The signal counts of the genes for mesophyll protoplasts were derived from previously published microarray data[61]. *LHCB2.2* (*PHOTOSYSTEM II LIGHT HARVESTING COMPLEX GENE 2.2*) serves as a leaf-specific expression control. The control gene *UBQ10* is constitutively and highly expressed in roots, shoots and mesophyll protoplasts. Error bars, s.d., n=3 biological replicates from mesophyll protoplasts. **e**, Nitrate induction of the endogenous *NIR* gene as a primary nitrate responsive marker gene in seedlings and mesophyll protoplasts. *NIR* expression was quantified by RT-qPCR analysis. *Arabidopsis* seedlings or mesophyll protoplasts were treated with 10 mM KCl or KNO_3 for 2 h. Error bars, s.d., n=3 biological replicates. **f, g**, Time-lapse images of nitrate stimulated Ca^{2+} signalling in roots of intact transgenic GCaMP6 plants. The entire time-lapse recording of Ca^{2+} signals stimulated by 10 mM KCl or KNO_3 in the root tip (**f**) or the elongated region (**g**) was presented in Supplementary Video 3 and 4. Seedlings were grown on basal medium without nitrogen for 4 days and then stimulated by KCl or KNO_3. Scale bar, 10 μm. The experiments were repeated three times with 10 seedlings for each treatment with consistent results. Source data for **d**, **e** can be found in Supplementary Information.
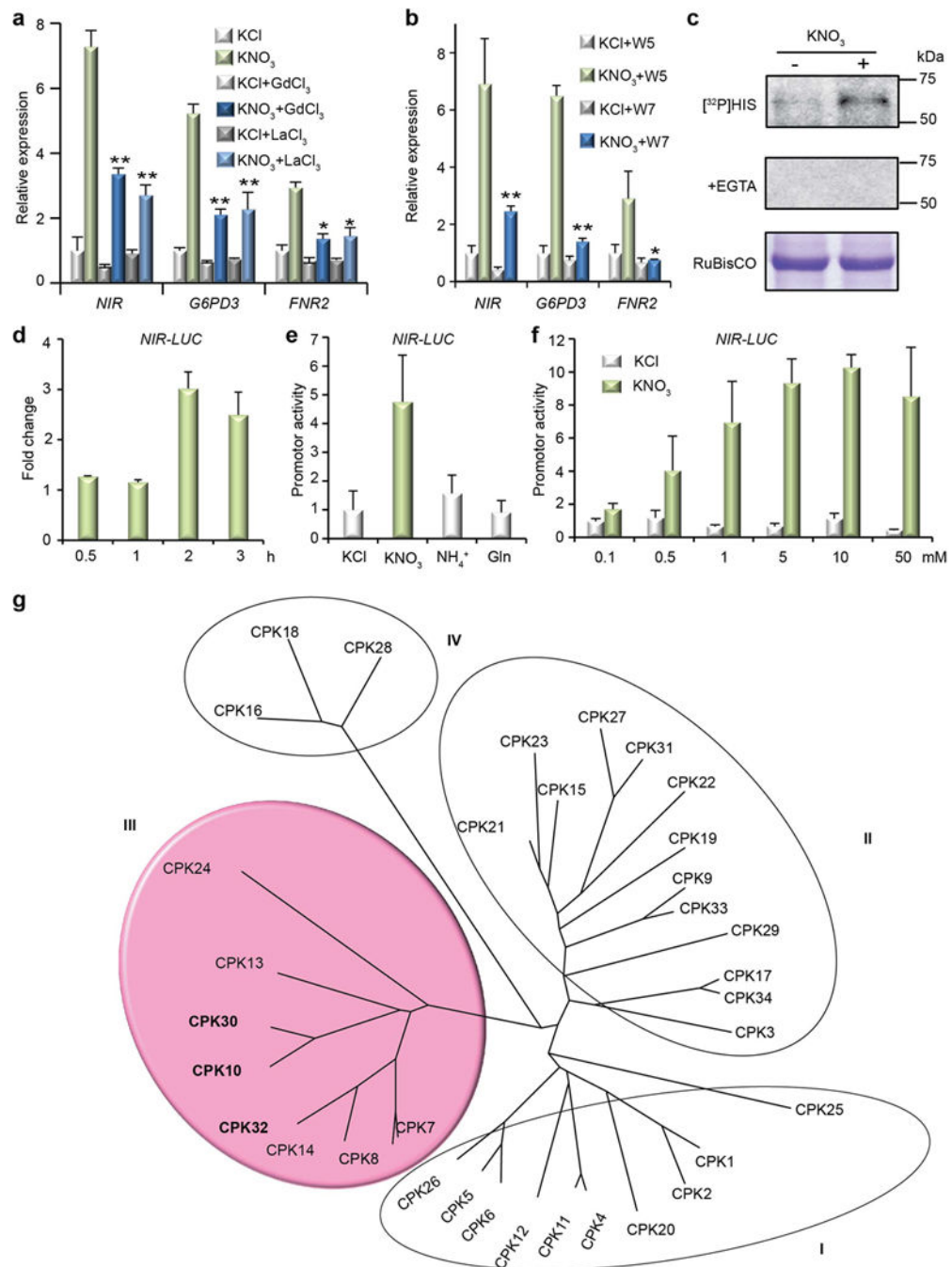
Extended Data Figure 2. Calcium mediates nitrate response in both seedlings and mesophyll protoplasts

a, Ca^{2+} channel blockers diminish primary nitrate responsive transcription. RT-qPCR analyses with 7-day-old seedlings. KNO_3, 0.5 mM, 15 min. Error bars, s.d., n=3 biological replicates, **$P < 0.0001$ and *$P < 0.05$ (two-way ANOVA with Tukey's multiple comparisons test). **b**, An antagonist of Ca^{2+} sensors (W7) inhibits primary nitrate responsive transcription. Error bars, s.d., n=3 biological replicates, **$P < 0.0001$ and *$P < 0.05$ (two-way ANOVA with Tukey's multiple comparisons test). **c**, Nitrate stimulates putative endogenous

CPKs in an in-gel kinase assay. KNO$_3$, 10 mM, 10 min. [^{32}P]HIS, histone phosphorylation. **d**, Time-course analysis of NIR-LUC activity in response to nitrate induction. Mesophyll protoplasts co-transfected with *NIR-LUC* and *UBQ10-GUS* (as the internal control) were incubated in WI buffer for 4 h and then induced by 0.5 mM KCl, or KNO$_3$ for 0.5, 1, 2, and 3 h. The fold change is calculated relative to the value of KCl treatment at each time point. Error bars, s.d., n=3 biological replicates. **e**, Nitrate-specific induction of *NIR-LUC* expression. Transfected mesophyll protoplasts were incubated in WI buffer for 4 h and then induced by 0.5 mM KCl or different nitrogen sources for 2 h. Error bars, s.d., n=3 biological replicates. **f**, Sensitive regulation of *NIR-LUC* by nitrate. Transfected mesophyll protoplasts were incubated in WI buffer for 4 h and then induced by different concentration of KCl or KNO$_3$ for 2 h. Error bars, s.d., n=3 biological replicates. **g**, Relation tree of Arabidopsis CPK proteins. The relation tree was generated by MEGA6 (Molecular Evolutionary Genetics Analyses 6) using the complete protein sequences of CPKs. The subgroup III CPKs that enhanced *NIR-LUC* activity more than two folds are highlighted. Genes encoding CPK14 and CPK24 are not expressed in mesophyll cells. Source data for **a**, **b**, **d**, **e**, **f** can be found in Supplementary Information.
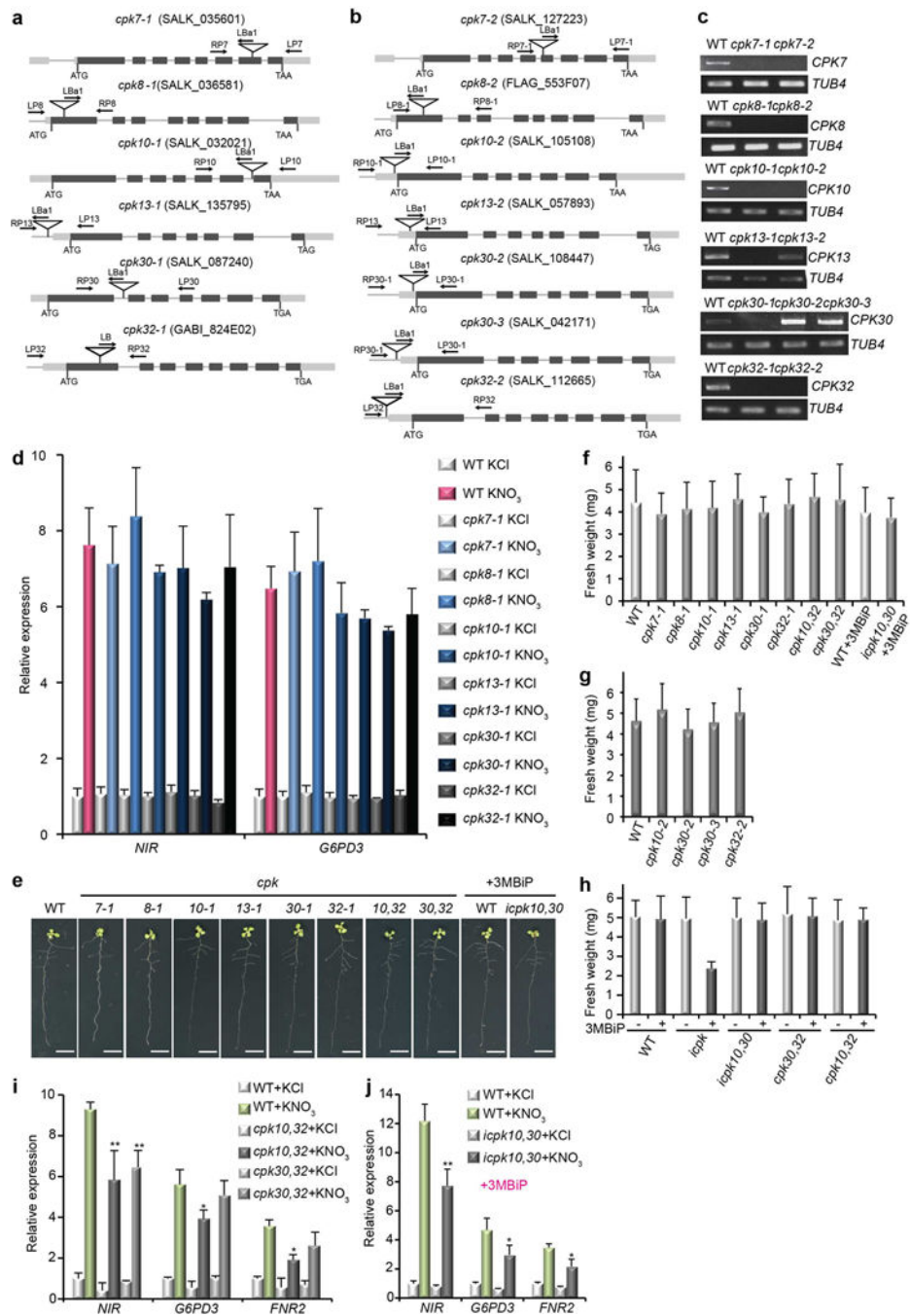
Extended Data Figure 3. Analyses of single, double *cpk*, and *icpk* mutants in subgroup III CPKs
a, **b**, The *cpk* T-DNA insertion lines. All *cpk* mutants were isolated and confirmed by PCR analysis of genomic DNA using gene specific primers and a T-DNA left border primer. Lines represent introns or promoters whereas dark and light grey boxes represent exons and untranslated regions, respectively. Arrows represent primers used for genotyping (see Supplementary Table 4). **c**, RT-PCR analysis of *CPK* transcripts in *cpk* mutants. *TUB4*, the housekeeping gene control. **d**, Analyses of nitrate responsive marker gene expression in *cpk* mutants. Seedlings (7-day-old) were induced by 0.5 mM KCl or KNO$_3$ for 15 min. Relative

expression of nitrate responsive marker genes was analysed by RT-qPCR and normalized to the expression of *UBQ10*. The relative expression level is calculated relative to the value of wild type (WT) treated with KCl. Error bars, s.d., n=3 biological replicates. **e**, Single and double *cpk* mutants lack overt phenotype. Plants were germinated and grown on the ammonium succinate medium for 3 days and then transferred to basal medium plates supplemented with 5 mM KNO_3 for 6 days. For analysing the chemical analogue sensitive mutants, WT and *icpk10,30* were transferred to basal medium plates supplemented with 5 mM KNO_3 and 1 μM 3MBiP for 6 days, and 3MBiP was reapplied every 2 days after transfer. Scale bar, 1 cm. The images are representative of 10 seedlings. **f, g**, The average fresh weight of 9-day-old single and double *cpk* mutants. Error bars, s.d., n=12 seedlings. **h**, The average fresh weight of 9-day-old double *cpk* mutants and *icpk* supplemented with or without 3MBiP. Error bars, s.d., n=12 seedlings. **i, j** Primary nitrate responsive gene expression is reduced in *cpk* double mutants. RT-qPCR analyses with 7-day-old seedlings. KNO_3, 0.5 mM, 15 min. Error bars, s.d., n=3 seedlings. **P< 0.0001 and *P< 0.05 (two-way ANOVA with Tukey's multiple comparisons test). Source data for **d**, **i**, **j** can be found in Supplementary Information.

a

CPK-regulated 44 / 35

b

Legend:
- Transporters (NO₃⁻, NH₄⁺ or AA)
- N metabolism
- Signalling
- Transcription factors
- Hormones
- Other transporters
- Protein degradation
- Metabolism
- Stress
- Photosynthesis
- Others
- Unknown

c Up-regulated genes

Functional Category	Gene Count	Fold Enrichment	p-value
OPP	8	32.9	8.60E-11
Transporters (NO₃⁻, NH₄⁺ or AA)	12	10.1	3.03E-09
Glycolysis	4	6.4	3.12E-03
N metabolism	10	4.4	8.82E-05
CHO metabolism	6	3.4	6.87E-03
Hormone metabolism	14	3.3	8.54E-05
Other transporters	20	2.9	1.77E-05
Transcription factor	47	2.4	7.14E-09
Metabolism	25	1.9	6.84E-04
Stress	20	1.8	5.30E-03
Signalling	18	1.7	1.13E-02

d Down-regulagted genes

Functional Category	Gene Count	Fold Enrichment	p-value
Transporters (NO₃⁻, NH₄⁺ or AA)	2	10.1	1.57E-02
Hormone metabolism	5	7.1	6.09E-04
N metabolism	2	5.3	4.83E-02
Other transporters	4	3.5	2.17E-02

e

f

WT+KCl, WT+KNO₃, icpk+KCl, icpk+KNO₃

g

Gene	WT Fold Induction KNO₃/KCl	SD	icpk Fold Induction KNO₃/KCl	SD	q-value*
FNR1	13.3	0.74	3.8	0.87	1.35E-04
NRT2.2	13.8	5.26	5.7	2.04	4.06E-04
LHT1	3.2	1.08	0.9	0.50	1.91E-01
TPPB	13.2	2.46	5.4	0.78	4.81E-04
GDH3	5.9	2.77	1.2	0.36	2.72E-02
NPH3	4.2	1.17	1.3	0.78	1.52E-01
CYP735A2	4.8	0.95	2.4	0.49	1.91E-01
NLP3	4.0	1.32	2.8	0.39	3.52E-01
HRS1	18.6	7.24	10.3	3.10	4.06E-04
TGA4	2.9	1.02	1.8	0.65	3.52E-01

*:FDR (False Discovery Rate). Two-stage step-up method of Benjamini, Krieger and Yekutieli
n=3 biological replicates

Extended Data Figure 4. RNA-Seq, qRT-PCR data analyses and functional classification
Biological triplicate RNA-seq experiments were performed and analysed with DESeq2. **a**, Nitrate-CPK down-regulated genes. Dark grey, nitrate-CPK target genes (q 0.05). **b**, Classification of nitrate-CPK down-regulated genes. The MapMan functional categories for nitrate down-regulated genes are presented. **c**, Enriched functional categories of nitrate up-regulated genes. **d**, Enriched functional categories of nitrate down-regulated genes. The fold enrichment is calculated as follows: (Number of Classified_input_set/Number of total_input_set) / (Number of Classified_reference_set/Number of total_reference_set). The

p-value is calculated in Excel using a hypergeometric distribution test. The categories were sorted by fold enrichment with a *p* 0.05 cut-off. **e**, Nitrate-CPK target genes regulate nitrogen transport and metabolism. **f**, RT-qPCR analyses of nitrate-CPK target genes in eight functional classes in seedlings. KNO_3, 10 mM, 15 min. Error bars, s.d., n=3 biological replicates. *NITRATE REDUCTASE1/2 (NIA1/2), NIR, NITRATE TRANSPORTER2.1/2.2 (NRT2.1/2.2), G6PD2/3, GLUTAMINE SYNTHETASE (GLN), GLUTAMATE DEHYDROGENASE3 (GDH3), UROPORPHYRINOGEN III METHYLTRANSFERASE1 (UPM1), FERREDOXIN3 (FD3)* and *FNR1/2*, were regulated by CPK10/30/32[1,3,4,12,17,18,21,32]. TF genes, *NLP3, HRS1 (HYPERSENSITIVITY TO LOW PI-ELICITED PRIMARY ROOT SHORTENING1)* and *TGA4 (TGACG MOTIF-BINDING FACTOR 4)* were primary nitrate-CPK target genes[12,17,18,20,24]. **g**, The fold changes of expression levels of nitrate up-regulated genes in WT and *icpk* listed in **f**. The table provided the source data for the histograms presented in **f**. n=3 biological replicates.

**Extended Data Figure 5. Primary nitrate up-regulated genes are present in diverse experimental systems**

Venn diagrams (http://www.cmbi.ru.nl/cdd/biovenn/) were used to present the comparison and overlaps between the list of primary nitrate up-regulated genes defined in this study and the nitrate up-regulated genes at 20 min defined by previously published gene sets from Wang et al., 2003[1], Krouk et al., 2010[15], and Marchive et al., 2013[18]. Red, 394 nitrate up-regulated genes identified in this study with a $\log_2 \geq 1$ and $q \leq 0.05$ cut-off; Light red, 992 nitrate up-regulated genes in this study with a $q \leq 0.05$ cut-off; Dark blue, 338 nitrate up-regulated genes from Wang et al., 2003[1] with a $\log_2 \geq 1$ cut-off for both biological duplicate data sets; Green, 366 nitrate up-regulated genes from Krouk et al., 2010[15] data set with a $\log_2 \geq 1$ cut-off; Light blue, 227 nitrate up-regulated genes from Marchive et al., 2013[18] with a $\log_2 \geq 1$ cut-off. Gene numbers in each group and the percentage of overlapped nitrate up-regulated genes in previously published data sets are shown.
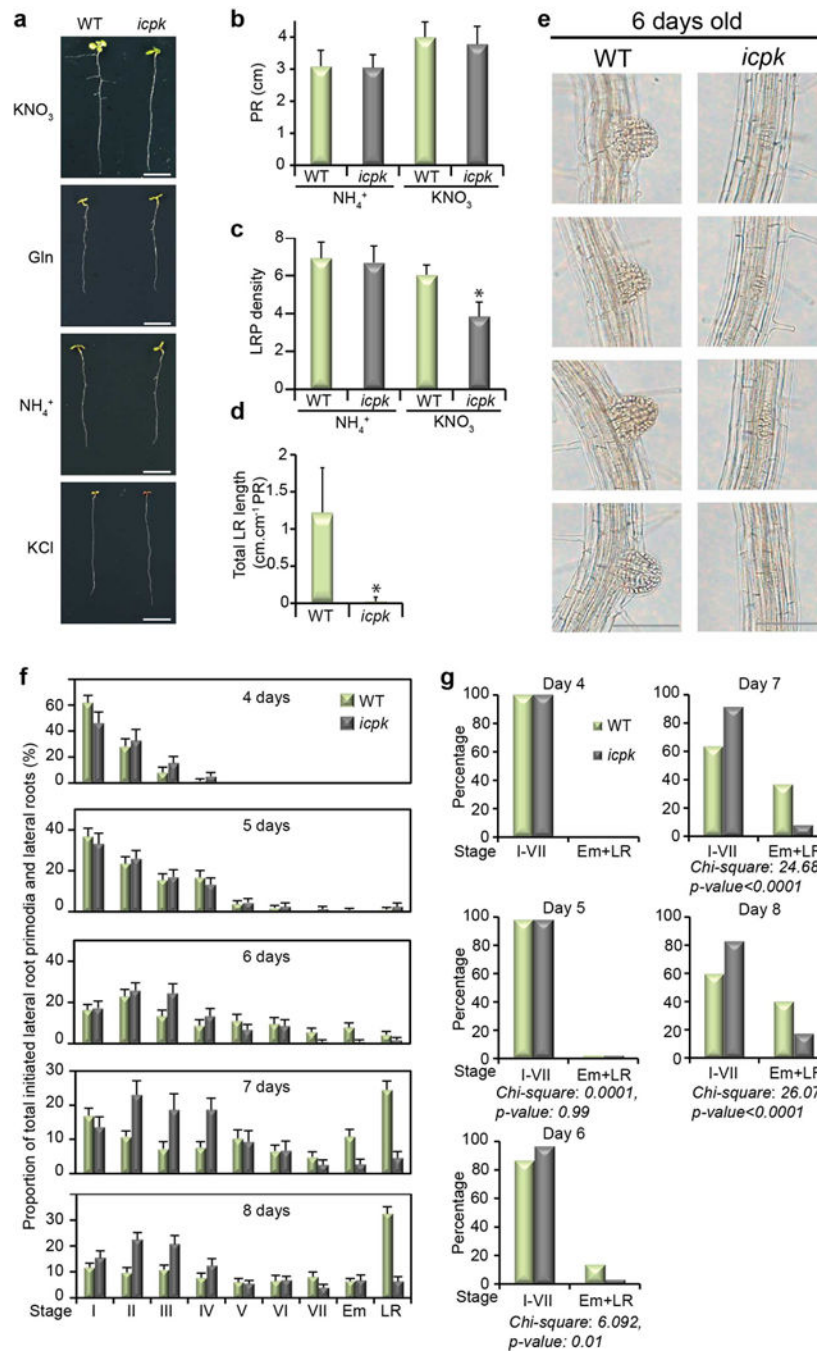
Extended Data Figure 6. Quantitative analyses of root growth phenotype in WT and *icpk* in response to ammonium and nitrate

a, The *icpk* mutant displays defects in nitrate-stimulated lateral root establishment. WT and the *icpk* mutant were germinated and grown on the ammonium succinate medium for 3 days, and then transferred to the plate supplemented with 5 mM KNO_3 or 2.5 mM ammonium succinate (NH^{4+}) or 5 mM KCl or 5 mM glutamine (Gln) in the presence of 1 μM 3MBiP for 5 days. Scale bar, 1 cm. The images are representative of 6 seedlings. **b**, Primary root (PR) length was similar in 8-day-old seedlings of WT and *icpk*. Error bars, s.d., n=16

seedlings. **c**, Lateral root primordium (LRP) density decreased significantly in 8-day-old *icpk* in response to nitrate. Error bars, s.d., n=15 seedlings, Student's t-test, *$p < 0.05$. **d**, Lateral root length was dramatically reduced in *icpk* in the presence of nitrate. Error bars, s.d., n=10 seedlings, Student's t-test, *$p < 0.05$. **e**, The development of lateral roots is severely retarded in *icpk*. The developmental stages of the third lateral root in WT and *icpk* induced by nitrate for 3 days (6-day-old) are shown. Scale bar, 100 μm. The images are representative of 6 seedlings. **f**, Time-course analyses of *icpk* defects in nitrate-specific lateral root development I-VII lateral root developmental stages[44]. Em, emerged primordia. LR, lateral root. Error bars, s.e.m., n=16 seedlings. **g**, Chi-square test of WT and *icpk* lateral root development. WT and *icpk* were compared on two categories, early lateral root development stages before emergence (stage I to VII) and stages afterwards (Em+LR). The low *p*-value indicates the high level of association between the genotype and development stages.
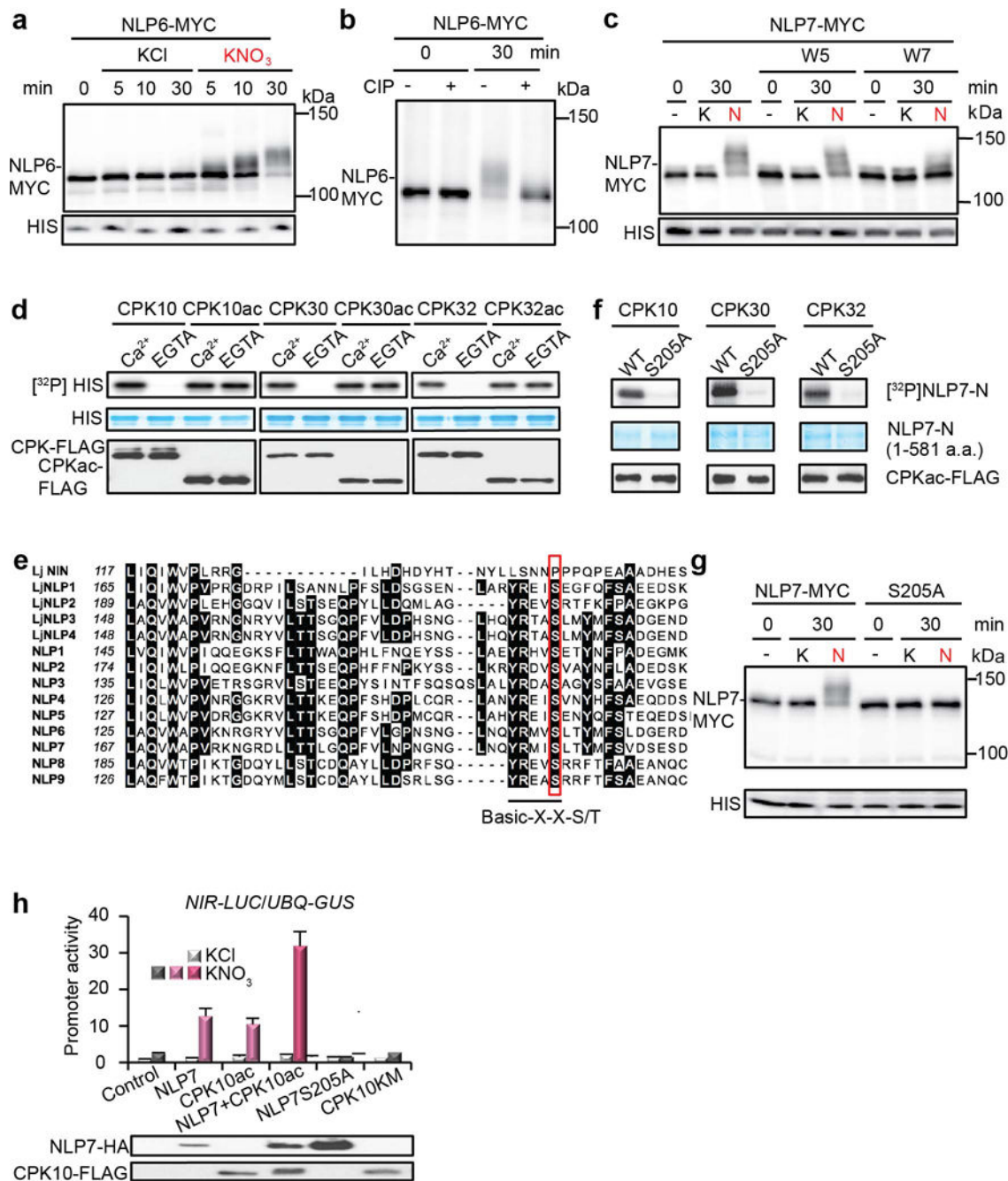
Extended Data Figure 7. Nitrate-induced NLP phosphorylation

a, Nitrate-induced mobility shift of MYC-tagged NLP6. Transgenic seedlings expressing MYC-tagged NLP6 were grown in liquid medium containing 0.5 mM ammonium succinate as a sole nitrogen source for 4 days and then treated with 10 mM KCl or KNO_3 for indicated periods. Immunoblot analysis was carried out with proteins extracted from the seedlings using anti-MYC (MYC) and anti-histone H3 (HIS) antibodies. **b,** Effect of alkaline phosphatase treatment on mobility shift of MYC-tagged NLP6. Proteins from seedlings treated with 10 mM KNO_3 for 0 or 30 min were subjected to calf-intestinal alkaline phosphatase (CIP) treatment. The experiments were repeated twice with consistent results. **c,**
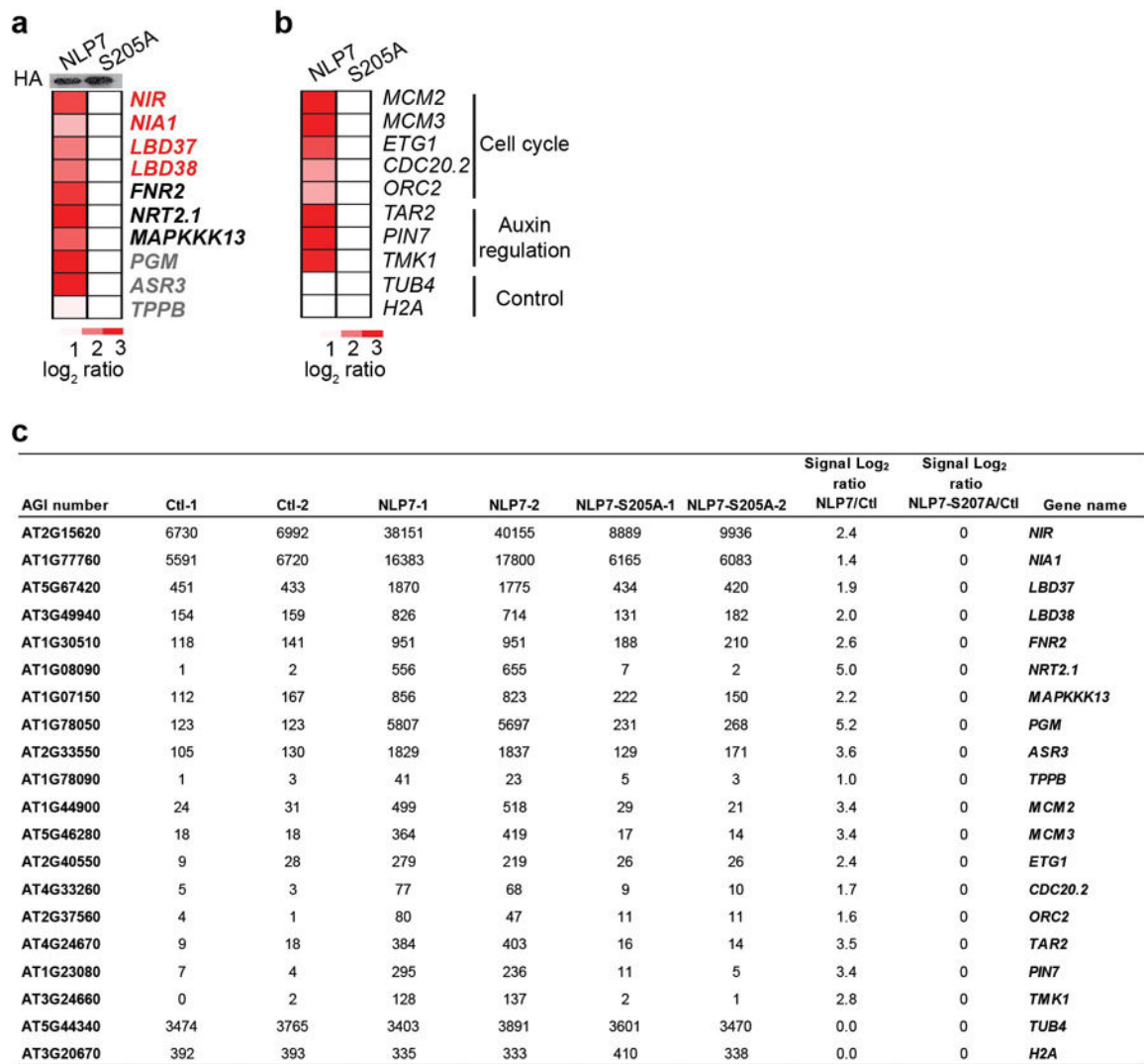
An antagonist of Ca^{2+} sensors (W7) diminished nitrate-triggered phosphorylation of NLP7. **d**, Phosphorylation of histone by CPK10/30/32 is Ca^{2+}-dependent. **e.** Alignment of the amino acid sequences around the conserved CPK phosphorylation site in all NLPs from *Arabidopsis thaliana* and *Lotus japonicus*. Conserved amino acid residues are indicated by black boxes. The CPK phosphorylation motif indicated by an underline was identified by multiple web-based bioinformatics tools and literature analysis[62-67] with a candidate serine (S205 in NLP7) that is uniquely conserved in nine *Arabidopsis* NLPs and four orthologous *Lotus japonicus* NLPs (outlined in red), but not in *Lj*NIN (NODULE INCEPTION). *Lj*NIN, a variant of NLP, which evolved specifically for symbiotic nitrogen fixation in legumes, lacks CPK phosphorylation site. **f**, S205 in NLP7 is the CPK10/30/32 phosphorylation site. **g**, Nitrate-induced mobility shift was abolished for NLP7(S205A). **h**, NLP7 and CPK10ac overexpression showed similar synergism with nitrate for *NIR-LUC* activation in protoplast transient assays. NLP7 or CPK10ac alone was not effective to enhance *NIR-LUC* expression without nitrate. CPK10KM lacking kinase activity and NLP7(S205A) lacking the CPK10,30,32 phosphorylation site served as negative controls. NLP7 or CPK10ac protein expression was detected by immunoblot analyses before dividing protoplasts equally and treated with 0.5 mM KCl or KNO_3 for 2 h. *UBQ10-GUS* is a transient expression control. Error bars, s.d., n=5 biological replicates.
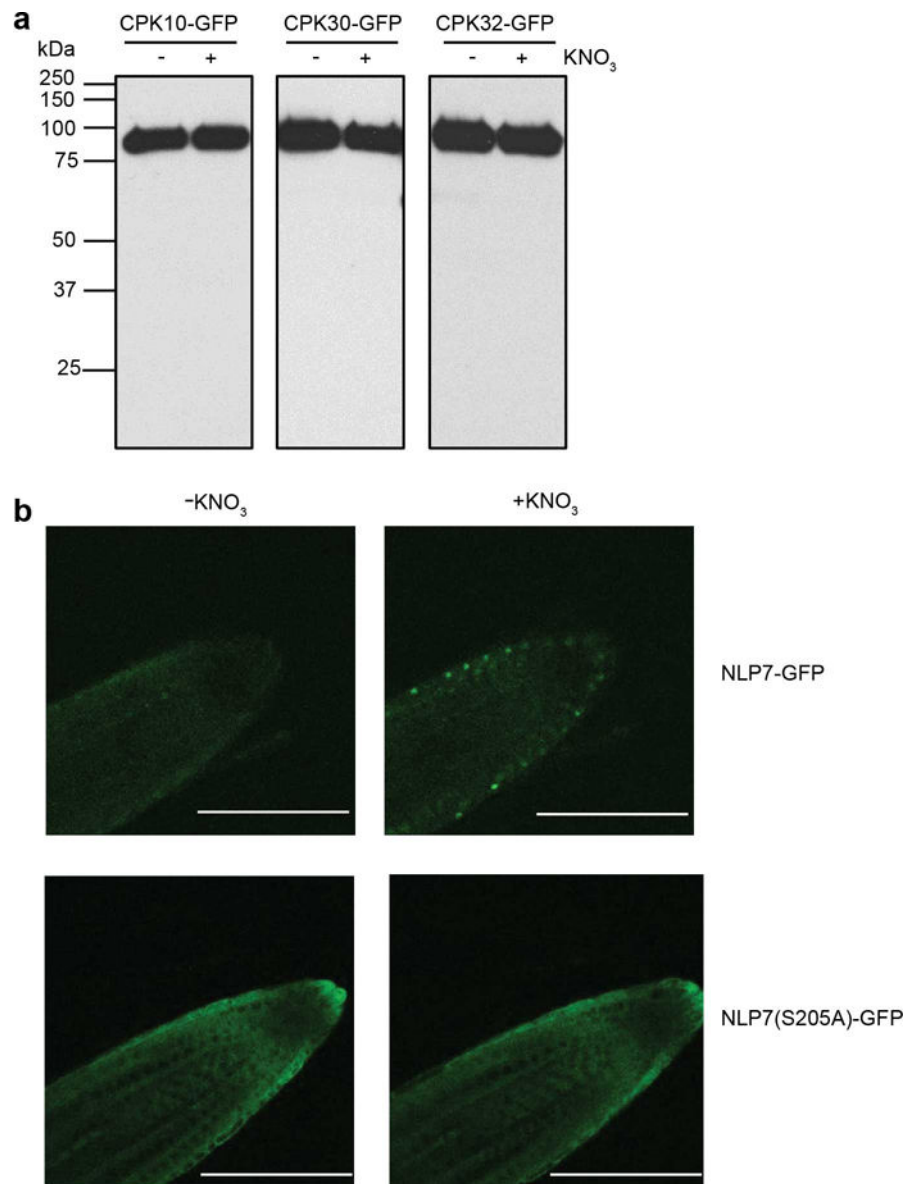
Extended Data Figure 8. The CPK phosphorylation residue S205 is required for NLP7 nuclear retention triggered by nitrate at the plant root tip

a, CPK-GFPs are not processed in response to nitrate. Proteins from CPK-GFP transfected protoplasts were analysed by immuno-blots with an anti-GFP antibody. **b**, Confocal image of NLP7-GFP or NLP7(S205A)-GFP in transgenic *nlp7-1* complementation plants in response to nitrate. GFP images recorded at 0 min or 8 min after 10 mM KNO_3 induction were shown. Scale bar, 100 μm. The experiments were repeated three times with 10 seedlings for each line with consistent results.

a

	NLP7	S205A
HA		

Genes: NIR, NIA1, LBD37, LBD38, FNR2, NRT2.1, MAPKKK13, PGM, ASR3, TPPB

log₂ ratio: 1 2 3

b

	NLP7	S205A

Genes: MCM2, MCM3, ETG1, CDC20.2, ORC2 (Cell cycle); TAR2, PIN7, TMK1 (Auxin regulation); TUB4, H2A (Control)

log₂ ratio: 1 2 3

c

AGI number	Ctl-1	Ctl-2	NLP7-1	NLP7-2	NLP7-S205A-1	NLP7-S205A-2	Signal Log₂ ratio NLP7/Ctl	Signal Log₂ ratio NLP7-S207A/Ctl	Gene name
AT2G15620	6730	6992	38151	40155	8889	9936	2.4	0	NIR
AT1G77760	5591	6720	16383	17800	6165	6083	1.4	0	NIA1
AT5G67420	451	433	1870	1775	434	420	1.9	0	LBD37
AT3G49940	154	159	826	714	131	182	2.0	0	LBD38
AT1G30510	118	141	951	951	188	210	2.6	0	FNR2
AT1G08090	1	2	556	655	7	2	5.0	0	NRT2.1
AT1G07150	112	167	856	823	222	150	2.2	0	MAPKKK13
AT1G78050	123	123	5807	5697	231	268	5.2	0	PGM
AT2G33550	105	130	1829	1837	129	171	3.6	0	ASR3
AT1G78090	1	3	41	23	5	3	1.0	0	TPPB
AT1G44900	24	31	499	518	29	21	3.4	0	MCM2
AT5G46280	18	18	364	419	17	14	3.4	0	MCM3
AT2G40550	9	28	279	219	26	26	2.4	0	ETG1
AT4G33260	5	3	77	68	9	10	1.7	0	CDC20.2
AT2G37560	4	1	80	47	11	11	1.6	0	ORC2
AT4G24670	9	18	384	403	16	14	3.5	0	TAR2
AT1G23080	7	4	295	236	11	5	3.4	0	PIN7
AT3G24660	0	2	128	137	2	1	2.8	0	TMK1
AT5G44340	3474	3765	3403	3891	3601	3470	0.0	0	TUB4
AT3G20670	392	393	335	333	410	338	0.0	0	H2A

Extended Data Figure 9. Nitrate enhancement of proliferation in the lateral root primordia

a, b, S205 is crucial for NLP7-mediated transcriptional activation of target genes with diverse functions. Genome-wide transcriptional profiling by RNA-Seq was performed with mesophyll protoplasts expressing NLP7-HA or NLP7(S205A)-HA or the control plasmid for 4.5 h. Red, NLP7 target genes identified by both ChIP-chip[18] and DAP-seq[68]; Black, ChIP-chip only; Grey, DAP-seq only. **c,** Normalized HTSeq read counts of NLP7-activated genes (listed in a,b) from RNA-Seq experiments. Normalized read counts of NLP7-activated genes calculated as the original HTseq counts divided by the normalization factors were extracted after DESeq2 analysis.
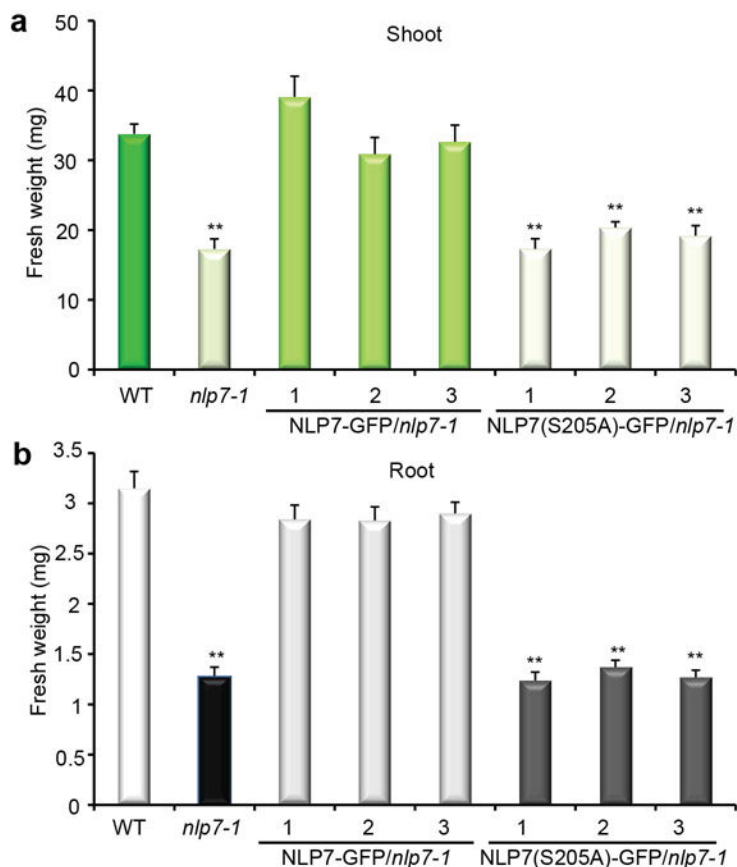
Extended Data Figure 10. Complementation analyses of *nlp7-1* with NLP7-GFP or NLP7(S205A)-GFP in transgenic *Arabidopsis* plants

a, The shoot fresh weight of WT, *nlp7-1*, NLP7-GFP/*nlp7-1* and NLP7(S205A)-GFP/*nlp7-1* shoots. Error bars, s.e.m., n=10 seedlings. **p 0.0001 versus WT control (one-way ANOVA with Tukey's multiple comparisons test). Plants were grown on 25 mM KNO_3 medium for 21 days. Data of three independent complement lines were presented. **b**, The root fresh weight of 11-day-old WT, *nlp7-1*, NLP7-GFP/*nlp7-1* and NLP7-S205A-GFP/*nlp7-1*. Seedlings were germinated on the ammonium succinate medium for 3 days and then transferred to the plates supplemented with 5 mM KNO_3 for 8 days. Error bars, s.e.m., n=10 seedlings. **p 0.0001 versus WT control (one-way ANOVA with Tukey's multiple comparisons test).

Supplementary Material

Refer to Web version on PubMed Central for supplementary material.

Acknowledgments

References

1. Wang R, Okamoto M, Xing X, Crawford NM. Microarray analysis of the nitrate response in Arabidopsis roots and shoots reveals over 1,000 rapidly responding genes and new linkages to glucose, trehalose-6-phosphate, iron, and sulfate metabolism. Plant Physiol. 2003; 132:556–67. [PubMed: 12805587]

2. Sheen J. Master regulators in plant glucose signaling networks. J Plant Biol. 2014; 57:67–79. [PubMed: 25530701]

3. Scheible WR, et al. Genome-wide reprogramming of primary and secondary metabolism, protein synthesis, cellular growth processes, and the regulatory infrastructure of Arabidopsis in response to nitrogen. Plant Physiol. 2004; 136:2483–99. [PubMed: 15375205]

4. Nunes-Nesi A, Fernie AR, Stitt M. Metabolic and signaling aspects underpinning the regulation of plant carbon nitrogen interactions. Mol Plant. 2010; 3:973–96. [PubMed: 20926550]

5. Xiong Y, et al. Glucose-TOR signalling reprograms the transcriptome and activates meristems. Nature. 2013; 496:181–6. [PubMed: 23542588]

6. Kiba T, Krapp A. Plant nitrogen acquisition under low availability: regulation of uptake and root architecture. Plant Cell Physiol. 2016; 57:707–14. [PubMed: 27025887]

7. Efeyan A, Comb WC, Sabatini DM. Nutrient-sensing mechanisms and pathways. Nature. 2015; 517:302–10. [PubMed: 25592535]

8. Rebsamen M, et al. SLC38A9 is a component of the lysosomal amino acid sensing machinery that controls mTORC1. Nature. 2015; 519:477–81. [PubMed: 25561175]

9. Bouguyon E, et al. Multiple mechanisms of nitrate sensing by Arabidopsis nitrate transceptor NRT1.1. Nature Plants. 2015; 1:15015. [PubMed: 27246882]

10. Ho CH, Lin SH, Hu HC, Tsay YF. CHL1 functions as a nitrate sensor in plants. Cell. 2009; 138:1184–94. [PubMed: 19766570]

11. Wang R, Xing X, Wang Y, Tran A, Crawford NM. A genetic screen for nitrate regulatory mutants captures the nitrate transporter gene NRT1.1. Plant Physiol. 2009; 151:472–8. [PubMed: 19633234]

12. Konishi M, Yanagisawa S. Emergence of a new step towards understanding the molecular mechanisms underlying nitrate-regulated gene expression. J Exp Bot. 2014; 65:5589–600. [PubMed: 25005135]

13. Wang R, et al. Genomic analysis of the nitrate response using a nitrate reductase-null mutant of Arabidopsis. Plant Physiol. 2004; 136:2512–22. [PubMed: 15333754]

14. Castaings L, et al. The nodule inception-like protein 7 modulates nitrate sensing and metabolism in Arabidopsis. Plant J. 2009; 57:426–35. [PubMed: 18826430]

15. Krouk G, Mirowski P, LeCun Y, Shasha DE, Coruzzi GM. Predictive network modeling of the high-resolution dynamic plant transcriptome in response to nitrate. Genome Biol. 2010; 11:R123. [PubMed: 21182762]

16. Liu KH, McCormack M, Sheen J. Targeted parallel sequencing of large genetically-defined genomic regions for identifying mutations in Arabidopsis. Plant Methods. 2012; 8:12. [PubMed: 22462410]

17. Konishi M, Yanagisawa S. Arabidopsis NIN-like transcription factors have a central role in nitrate signalling. Nat Commun. 2013; 4:1617. [PubMed: 23511481]

18. Marchive C, et al. Nuclear retention of the transcription factor NLP7 orchestrates the early response to nitrate in plants. Nat Commun. 2013; 4:1713. [PubMed: 23591880]

19. Guan P, et al. Nitrate foraging by Arabidopsis roots is mediated by the transcription factor TCP20 through the systemic signaling pathway. Proc Natl Acad Sci U S A. 2014; 111:15267–72. [PubMed: 25288754]

20. Alvarez JM, et al. Systems approach identifies TGA1 and TGA4 transcription factors as important regulatory components of the nitrate response of Arabidopsis thaliana roots. Plant J. 2014; 80:1–13. [PubMed: 25039575]

21. Obertello M, Shrivastava S, Katari MS, Coruzzi GM. Cross-species network analysis uncovers conserved nitrogen-regulated network modules in rice. Plant Physiol. 2015; 168:1830–43. [PubMed: 26045464]

22. Hu HC, Wang YY, Tsay YF. AtCIPK8, a CBL-interacting protein kinase, regulates the low-affinity phase of the primary nitrate response. Plant J. 2009; 57:264–78. [PubMed: 18798873]

23. Leran S, et al. Nitrate sensing and uptake in Arabidopsis are enhanced by ABI2, a phosphatase inactivated by the stress hormone abscisic acid. Sci Signal. 2015; 8:ra43. [PubMed: 25943353]

24. Medici A, et al. AtNIGT1/HRS1 integrates nitrate and phosphate signals at the Arabidopsis root tip. Nat Commun. 2015; 6:6274. [PubMed: 25723764]

25. Vidal EA, Alvarez JM, Moyano TC, Gutierrez RA. Transcriptional networks in the nitrate response of Arabidopsis thaliana. Curr Opin Plant Biol. 2015; 27:125–132. [PubMed: 26247122]

26. Knight H, Trewavas AJ, Knight MR. Cold calcium signaling in Arabidopsis involves two cellular pools and a change in calcium signature after acclimation. Plant Cell. 1996; 8:489–503. [PubMed: 8721751]

27. Boudsocq M, et al. Differential innate immune signalling via Ca^{2+} sensor protein kinases. Nature. 2010; 464:418–22. [PubMed: 20164835]

28. Boudsocq M, Sheen J. CDPKs in immune and stress signaling. Trends Plant Sci. 2013; 18:30–40. [PubMed: 22974587]

29. Reddy AS, Ali GS, Celesnik H, Day IS. Coping with stresses: roles of calcium- and calcium/calmodulin-regulated gene expression. Plant Cell. 2011; 23:2010–32. [PubMed: 21642548]

30. Simeunovic A, Mair A, Wurzinger B, Teige M. Know where your clients are: subcellular localization and targets of calcium-dependent protein kinases. J Exp Bot. 2016; 67:3855–72. [PubMed: 27117335]

31. Ebert DH, Greenberg ME. Activity-dependent neuronal signalling and autism spectrum disorder. Nature. 2013; 493:327–37. [PubMed: 23325215]

32. Sakakibara H, Kobayashi K, Deji A, Sugiyama T. Partial characterization of the signaling pathway for the nitrate-dependent expression of genes for nitrogen-assimilatory enzymes using detached maize leaves. Plant and Cell Physiology. 1997; 38:837–843.

33. Riveras E, et al. The calcium ion is a second messenger in the nitrate signaling pathway of Arabidopsis. Plant Physiol. 2015; 169:1397–404. [PubMed: 26304850]

34. Forde BG. Glutamate signalling in roots. J Exp Bot. 2014; 65:779–87. [PubMed: 24151303]

35. Giehl RF, Gruber BD, von Wiren N. It's time to make changes: modulation of root system architecture by nutrient signals. J Exp Bot. 2014; 65:769–78. [PubMed: 24353245]

36. Chen TW, et al. Ultrasensitive fluorescent proteins for imaging neuronal activity. Nature. 2013; 499:295–300. [PubMed: 23868258]

37. Yuan F, et al. OSCA1 mediates osmotic-stress-evoked Ca^{2+} increases vital for osmosensing in Arabidopsis. Nature. 2014; 514:367–71. [PubMed: 25162526]

38. Charpentier M, et al. Nuclear-localized cyclic nucleotide-gated channels mediate symbiotic calcium oscillations. Science. 2016; 352:1102–5. [PubMed: 27230377]

39. Brandt B, et al. Calcium specificity signaling mechanisms in abscisic acid signal transduction in Arabidopsis guard cells. Elife. 2015; 4

40. Gan Y, Bernreiter A, Filleur S, Abram B, Forde BG. Overexpressing the ANR1 MADS-box gene in transgenic plants provides new insights into its role in the nitrate regulation of root development. Plant Cell Physiol. 2012; 53:1003–16. [PubMed: 22523192]

41. Liu Y, et al. Structural basis for selective inhibition of Src family kinases by PP1. Chem Biol. 1999; 6:671–8. [PubMed: 10467133]

42. Zhang C, et al. Structure-guided inhibitor design expands the scope of analog-sensitive kinase technology. ACS Chem Biol. 2013; 8:1931–8. [PubMed: 23841803]

43. Kiba T, Takei K, Kojima M, Sakakibara H. Side-chain modification of cytokinins controls shoot growth in Arabidopsis. Dev Cell. 2013; 27:452–61. [PubMed: 24286826]

44. Malamy JE, Benfey PN. Organization and cell differentiation in lateral roots of Arabidopsis thaliana. Development. 1997; 124:33–44. [PubMed: 9006065]

45. Chen TW, et al. Ultrasensitive fluorescent proteins for imaging neuronal activity. Nature. 2013; 499:295–300. [PubMed: 23868258]

46. Yoo SD, Cho YH, Sheen J. *Arabidopsis* mesophyll protoplasts: a versatile cell system for transient gene expression analysis. Nat Protoc. 2007; 2:1565–72. [PubMed: 17585298]

47. Xiang C, Han P, Lutziger I, Wang K, Oliver DJ. A mini binary vector series for plant transformation. Plant Mol Biol. 1999; 40:711–7. [PubMed: 10480394]

48. Clough SJ, Bent AF. Floral dip: a simplified method for *Agrobacterium*-mediated transformation of *Arabidopsis thaliana*. Plant J. 1998; 16:735–43. [PubMed: 10069079]

49. Guo J, et al. Involvement of *Arabidopsis* RACK1 in protein translation and its regulation by abscisic acid. Plant Physiol. 2011; 155:370–83. [PubMed: 21098678]

50. Kato Y, Konishi M, Shigyo M, Yoneyama T, Yanagisawa S. Characterization of plant eukaryotic translation initiation factor 6 (eIF6) genes: The essential role in embryogenesis and their differential expression in *Arabidopsis* and rice. Biochem Biophys Res Commun. 2010; 397:673–8. [PubMed: 20570652]

51. Alonso JM, et al. Genome-wide insertional mutagenesis of *Arabidopsis thaliana*. Science. 2003; 301:653–7. [PubMed: 12893945]

52. Kim D, et al. TopHat2: accurate alignment of transcriptomes in the presence of insertions, deletions and gene fusions. Genome Biol. 2013; 14:R36. [PubMed: 23618408]

53. Anders S, Pyl PT, Huber W. HTSeq–a Python framework to work with high-throughput sequencing data. Bioinformatics. 2015; 31:166–9. [PubMed: 25260700]

54. Love MI, Huber W, Anders S. Moderated estimation of fold change and dispersion for RNA-seq data with DESeq2. Genome Biol. 2014; 15:550. [PubMed: 25516281]

55. Van Verk MC, Hickman R, Pieterse CM, Van Wees SC. RNA-Seq: revelation of the messengers. Trends Plant Sci. 2013; 18:175–9. [PubMed: 23481128]

56. De Hoon MJ, Imoto S, Nolan J, Miyano S. Open source clustering software. Bioinformatics. 2004; 20:1453–4. [PubMed: 14871861]

57. Saldanha AJ. Java Treeview–extensible visualization of microarray data. Bioinformatics. 2004; 20:3246–8. [PubMed: 15180930]

58. Axelos M, Curic C, Mazzolini L, Bardet C, Lescure N. A protocol for transient gene expression in *Arabidopsis thaliana* protoplasts isolated from cell suspension cultures. Plant Physi Bioch. 1992; 30:123–128.

59. Aki T, Shigyo M, Nakano R, Yoneyama T, Yanagisawa S. Nano scale proteomics revealed the presence of regulatory proteins including three FT-Like proteins in phloem and xylem saps from rice. Plant Cell Physiol. 2008; 49:767–90. [PubMed: 18372294]

60. Aki T, Yanagisawa S. Application of rice nuclear proteome analysis to the identification of evolutionarily conserved and glucose-responsive nuclear proteins. J Proteome Res. 2009; 8:3912–24. [PubMed: 19621931]

61. Baena-Gonzalez E, Rolland F, Thevelein JM, Sheen J. A central integrator of transcription networks in plant stress and energy signalling. Nature. 2007; 448:938–42. [PubMed: 17671505]

62. Cheng SH, Willmann MR, Chen HC, Sheen J. Calcium signaling through protein kinases. The *Arabidopsis* calcium-dependent protein kinase gene family. Plant Physiol. 2002; 129:469–85. [PubMed: 12068094]

63. Curran A, et al. Calcium-dependent protein kinases from *Arabidopsis* show substrate specificity differences in an analysis of 103 substrates. Front Plant Sci. 2011; 2:36. [PubMed: 22645532]

64. Song C, et al. Systematic analysis of protein phosphorylation networks from phosphoproteomic data. Mol Cell Proteomics. 2012; 11:1070–83. [PubMed: 22798277]

65. Yaffe MB, et al. A motif-based profile scanning approach for genome-wide prediction of signaling pathways. Nat Biotechnol. 2001; 19:348–53. [PubMed: 11283593]

66. Soyano T, Shimoda Y, Hayashi M. NODULE INCEPTION antagonistically regulates gene expression with nitrate in Lotus japonicus. Plant Cell Physiol. 2015; 56:368–76. [PubMed: 25416287]

67. Suzuki W, Konishi M, Yanagisawa S. The evolutionary events necessary for the emergence of symbiotic nitrogen fixation in legumes may involve a loss of nitrate responsiveness of the NIN transcription factor. Plant Signal Behav. 2013; 8

68. O'Malley RC, et al. Cistrome and epicistrome features shape the regulatory DNA landscape. Cell. 2016; 165:1280–92. [PubMed: 27203113]
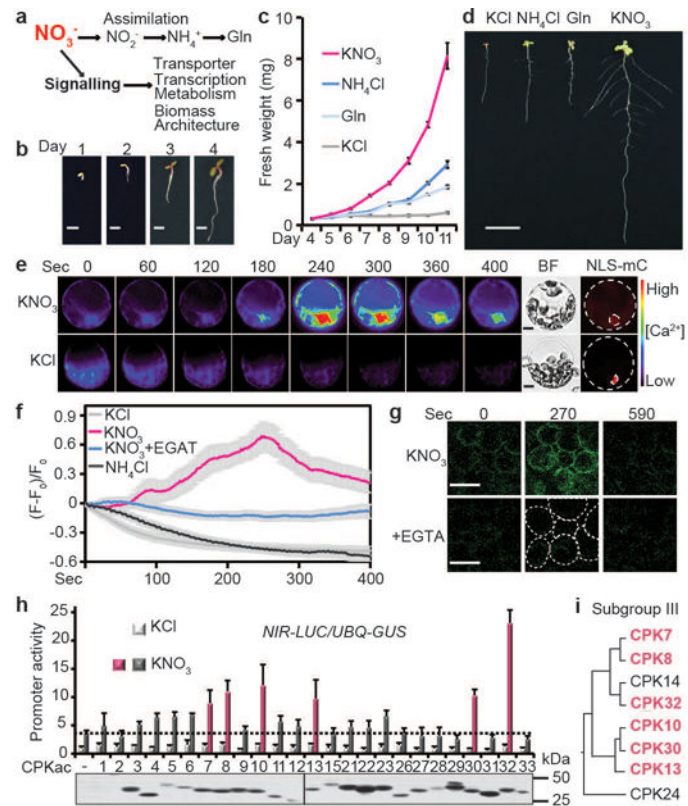
Figure 1. Nitrate triggers unique Ca^{2+}-CPK signalling

a, Dual nitrate functions in plants. **b**, *Arabidopsis* seedling development without exogenous nitrogen up to 4 days. Scale bar, 1 mm. The images are representative of 10 seedlings. **c, d**, Nitrate specifically promotes extensive shoot and root developmental programs. Different nitrogen sources (1 mM) were applied at day 5. Error bars, ± s.e.m., n=10 seedlings. Scale bar, 1 cm. **e**, Time-lapse images of Ca^{2+} signalling in the nucleus and cytosol stimulated by nitrate in mesophyll protoplasts expressing GCaMP6. KNO_3, 10 mM. BF, bright field. NLS-mC, nuclear HY5-mCherry. Scale bar, 10 μm. The images are representative of 10 protoplasts. **f**, Traces of GCaMP6 signals stimulated by nitrate in mesophyll protoplasts. KNO_3, 10 mM. $(F-F_0)/F_0$, relative fluorescence intensity. Error bars (grey areas, 199 error bars), ± s.e.m., n=10 protoplasts. **g**, Time-lapse images of Ca^{2+} signalling in mesophyll cells of cotyledons in GCaMP6 transgenic plants. KNO_3, 10 mM. Scale bar, 50 μm. The images are representative of 10 cotyledons. **h**, Subgroup III CPKac and nitrate synergistically activate *NIR-LUC* in protoplast transient assays. *UBQ10-GUS* is a control. KNO_3, 0.5 mM, 2 h. Error bars, s.d., n=3 biological replicates. Dash line: KNO_3 induction without CPKac. CPKac-FLAG expression was determined by immunoblot analyses. Source data can be found in Supplementary Information. **i**, The relation tree of subgroup III CPKs.
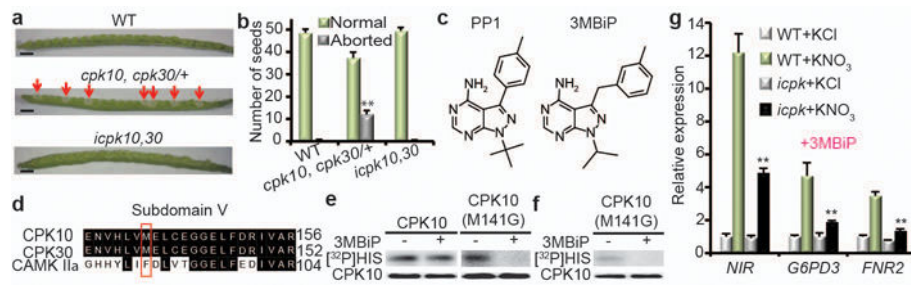
Figure 2. Chemical genetic analyses of CPK10/30/32

a, b, The embryo lethality of *cpk10,30* is rescued by CPK10(M141G) in *icpk10,30*. Arrows indicate aborted embryos. WT, wild type (Col-0). Scale bar, 1 mm. Error bars, s.d., n=10 siliques. **P<0.0001 (Chi-square). **c**, Chemical structure of 3MBiP derived from PP1. **d**, The gatekeeper residue in CPK10 and CPK30. **e, f**, The CPK10(M141G) activity isolated from protoplasts (**e**) or *icpk10,30* seedlings (**f**) is specifically inhibited by 3MBiP. [^{32}P]HIS, histone phosphorylation. **g**, Nitrate response is significantly diminished in the *icpk* triple mutant seedlings. Error bars, s.d., n=3 biological replicates. **$P<$ 0.0001 and *$P<$ 0.05 (two-way ANOVA with Tukey's multiple comparisons test). Source data can be found in Supplementary Information.
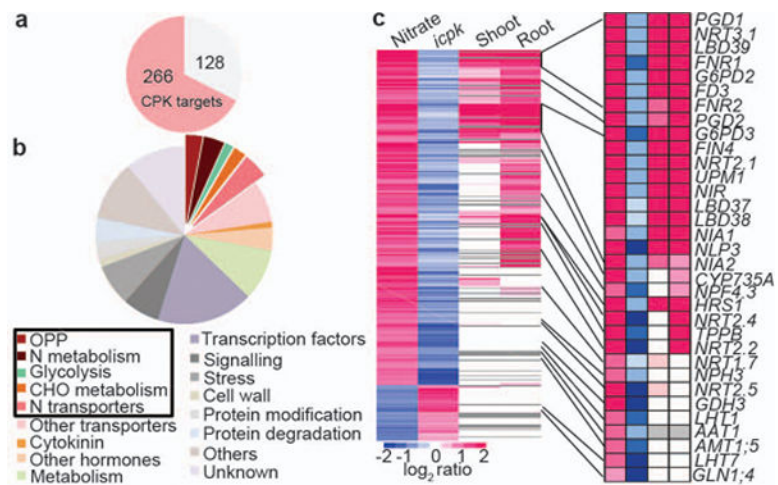
Figure 3. CPK10, CPK30 and CPK32 control primary nitrate responsive transcriptome
Transcriptome analyses of the primary nitrate response in WT and *icpk* seedlings by RNA-seq. **a**, Nitrate-CPK up-regulated target genes. Red, genes significantly affected in *icpk* (*q* 0.05). **b**, MapMan functional categories for nitrate-CPK up-regulated target genes. **c**, Hierarchical clustering analysis of nitrate-CPK target genes. Nitrate, primary nitrate responsive genes in WT. *icpk*, nitrate-CPK target genes. Shoot or Root, nitrate response genes identified by ATH1 genechips in shoots or roots[1]. Grey, gene probes not present on the ATH1 genechip.
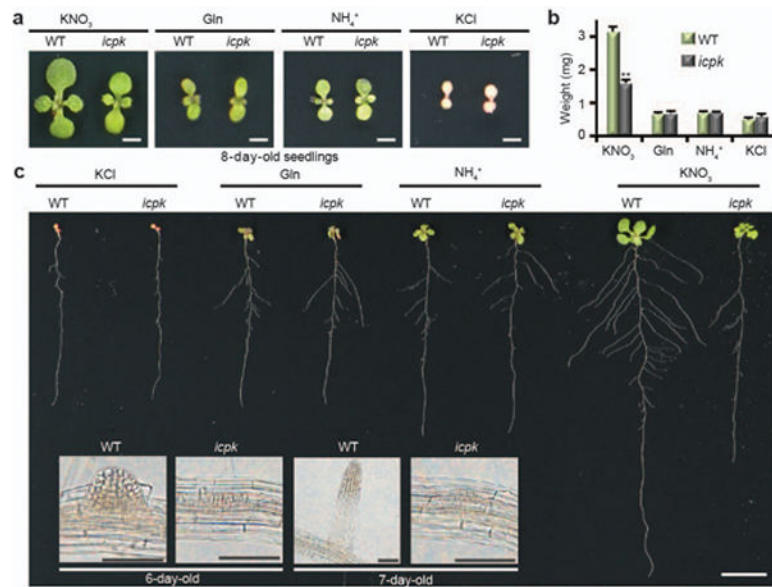
Figure 4. Dynamic Nitrate-CPK signalling orchestrates shoot and root development

a, b, The *icpk* mutant exhibits deficiency in nitrate-specific promotion of shoot development. Different nitrogen sources (5 mM KNO_3 or 2.5 mM ammonium succinate or 5 mM KCl or 1 mM Gln) and 1 μM 3MBiP were applied after 3 days on 2.5 mM $(NH_4)_2$-succinate to ensure even germination. Scale bar, 0.5 cm. Error bars, s.e.m., n=17 seedlings, **P< 0.0001 (two-way ANOVA with Tukey's multiple comparisons test). **c**, The root system architecture defects of *icpk* is nitrate specific. Scale bar, 1 cm. Inset: The third lateral root development induced by nitrate for 3 days (6-day-old) or 4 days (7-day-old) in WT and *icpk*. Scale bar, 100 μm. The images are representative of 10 seedlings.
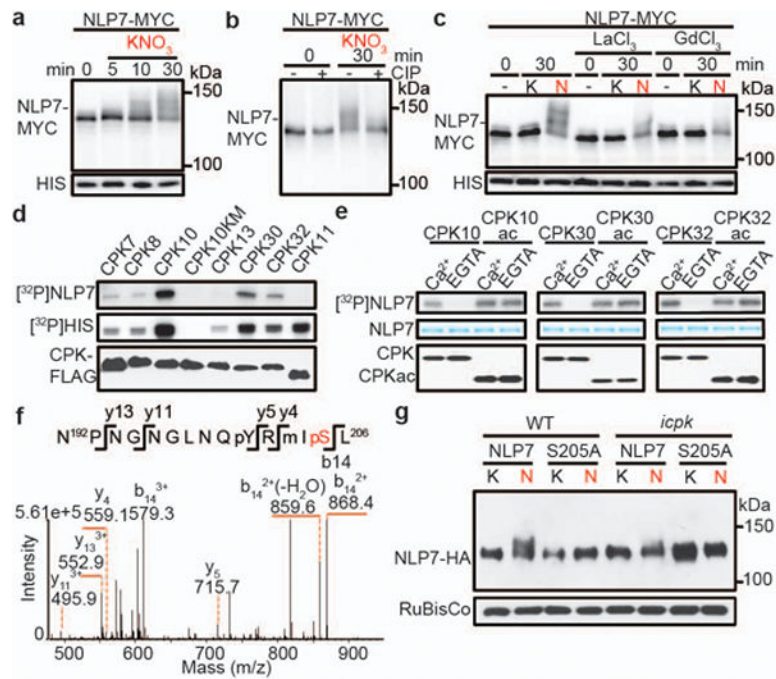
Figure 5. The CPK-NLP signalling connection
a, b, Nitrate triggers phosphorylation-dependent mobility shift of NLP7 in transgenic seedlings. 10 mM KCl (K) or KNO_3 (N). 10 mM. CIP, calf-intestinal alkaline phosphatase. **c,** Ca^{2+} channel blockers diminish nitrate-triggered NLP7 phosphorylation. **d,** CPK10/30/32 phosphorylate NLP7 *in vitro*. **e,** Phosphorylation of NLP7 by CPK10/30/32 is Ca^{2+}-dependent. **f,** Mass spectrometric analysis of NLP7 phosphorylation at Serine 205. **g,** Nitrate-induced phosphorylation of NLP7 at Serine 205 is abolished in *icpk*. 10 mM KCl (K) or KNO_3 (N) for 15 min.
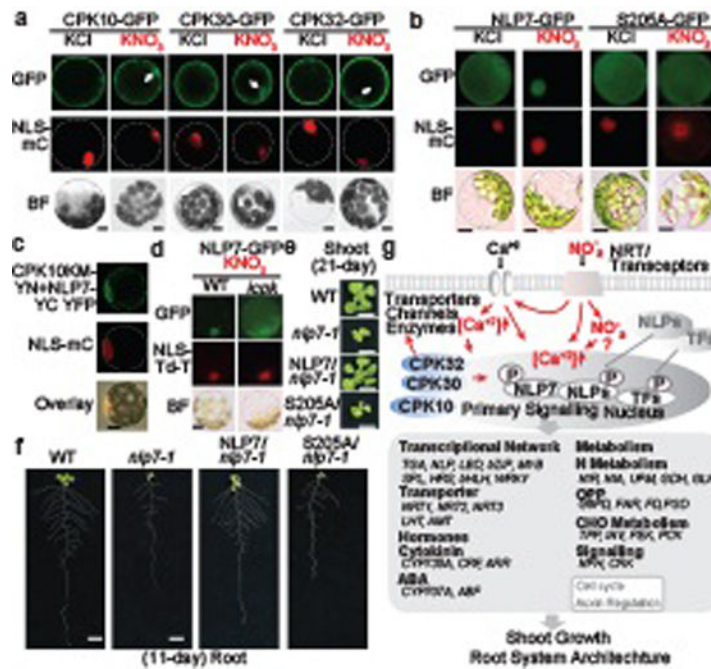
Figure 6. Nitrate-CPK-NLP signalling is crucial in nutrient-growth networks

a, CPK10/30/32 translocate to the nucleus in response to nitrate. KNO_3, 10 mM. Scale bar, 10 μm. NLS-mC, nuclear HY5-mCherry. BF, bright field. The images are representative of 8 protoplasts. **b**, Phosphorylation of S205 is required for nitrate-triggered nuclear retention of NLP7-GFP. KNO_3, 10 mM. Scale bar, 10 μm. The images are representative of 10 protoplasts. **c**, CPK10KM interacts with NLP7 in the nucleus in the BiFC assay. KNO_3, 10 mM. The images are representative of 8 protoplasts. **d**, Nitrate-triggered nuclear retention of NLP7-GFP is diminished in *icpk*. KNO_3, 10 mM. NLS-Td-T, nuclear Td-Tomato. The images are representative of 8 protoplasts. **e, f**, NLP7-GFP but not NLP7(S205A)-GFP complements the *nlp7* mutant. Scale bar, 1 cm. The images are representative of 20 seedlings. **g**, Nitrate-CPK-NLP signalling model.